ผลของสารตั้งต้นของแพลเลเดียมต่อปฏิกิริยาไฮโดรจิเนชันในวัฏภาคของเหลว บนตัวเร่งปฏิกิริยาแพลเลเดียมบนซิลิกา

นางสาว อรทัย ตั้งจิตวัฒนากร

วิทยานิพนธ์นี้เป็นส่วนหนึ่งของการศึกษาตามหลักสูตรปริญญาวิศวกรรมศาสตรมหาบัณฑิต
สาขาวิชาวิศวกรรมเคมี ภาควิชาวิศวกรรมเคมี
คณะวิศวกรรมศาสตร์ จุฬาลงกรณ์มหาวิทยาลัย
ปีการศึกษา 2547

ISBN: 974-53-1767-6

EFFECT OF PALLADIUM PRECURSORS ON LIQUID PHASE HYDROGENATION OVER SILICA-SUPPORTED PALLADIUM CATALYSTS

Miss Orathai Tangjitwattanakorn

A Thesis Submitted in Partial Fulfillment of the Requirements
for the Degree of Master of Engineering in Chemical Engineering
Department of Chemical Engineering
Faculty of Engineering
Chulalongkorn University
Academic Year 2004
ISBN: 974-53-1767-6

อรทัย ตั้งจิตวัฒนากร: ผลของสารตั้งต้นของแพลเลเดียมต่อปฏิกิริยาไฮโดรจิเนชันในวัฏภาคของเหลวบนตัวเร่งปฏิกิริยาแพลเลเดียมบนซิลิกา (EFFECT OF PALLADIUM PRECURSORS ON LIQUID PHASE HYDROGENATION OVER SILICA-SUPPORTED PALLADIUM CATALYSTS)
อ. ที่ปรึกษา: ดร. จูงใจ ปั้นประณต, อ. ที่ปรึกษา (ร่วม): ศาสตราจารย์ ดร.ปิยะสาร ประเสริฐธรรม 97 หน้า. ISBN: 974-53-1767-6

วิทยานิพนธ์นี้ศึกษาผลของสารตั้งต้นของแพลเลเดียมต่อคุณลักษณะ และสมบัติในการเร่งปฏิกิริยาของแพลเลเดียมบนตัวรองรับ SiO_2 และ MCM-41 ในปฏิกิริยาไฮโดรจิเนชันในวัฏภาคของเหลวของ 1-เฮกซีน โดยสารตั้งต้นแพลเลเดียมที่ใช้เตรียมตัวเร่งปฏิกิริยา ได้แก่ แพลเลเดียมไนเตท แพลเลเดียมคลอไรด์ และแพลเลเดียมอะซิเตท พบว่าการใช้สารตั้งต้นแพลเลเดียมคลอไรด์ จะทำให้ได้ขนาดผลึกแพลเลเดียมที่มีขนาดเล็กที่สุดเมื่อเทียบกับสารตั้งต้นตัวอื่นที่ใช้ในการศึกษา มีการกระจายตัวของแพลเลเดียมบนตัวรองรับซิลิกาที่สูง และมีความว่องไวในปฏิกิริยาไฮโดรจิเนชันของ 1-เฮกซีน สูงที่สุด เมื่อใช้สารตั้งต้นแพลเลเดียมชนิดเดียวกัน ค่าการกระจายตัวของ Pd และความว่องไวในปฏิกิริยาไฮโดรจิเนชันของ 1-เฮกซีนบนตัวรองรับ SiO_2และMCM-41 มีค่าใกล้เคียงกัน สำหรับการศึกษาการเสื่อมสภาพของตัวเร่งปฏิกิริยา พบว่าผลึกแพลเลเดียมเริ่มต้นที่มีขนาดเล็กมากไม่ถูกชะล้างในระหว่างทำปฏิกิริยา แต่ผลึกไม่มีความเสถียรต่อการ sintering โดยพบว่าผลึกมีขนาดใหญ่ขึ้นมาก ส่วนผลึกแพลเลเดียมที่เตรียมจากแพลเลเดียมไนเตทและแพลเลเดียมอะซิเตทเริ่มต้นมีขนาดใหญ่ถูกชะล้างประมาณ 30-50 เปอร์เซนต์หลังจากทำปฏิกิริยา แต่ผลึกจะมีความเสถียรต่อการ sintering มากกว่าผลึกเริ่มต้นขนาดเล็ก ทั้งนี้พบว่าตัวเร่งปฏิกิริยาแพลเลเดียมบนตัวรองรับ MCM-41 หลังจากผ่านการทำปฏิกิริยาไฮโดรจิเนชันของ 1-เฮกซีนในวัฏภาคของเหลวมีการกระจายตัวลดลงมากกว่าเมื่อเทียบกับตัวเร่งปฏิกิริยาบนตัวรองรับ SiO_2 อาจเนื่องมาจากมีการสลายตัวของโครงสร้าง MCM-41 บางส่วน ดังนั้นในงานนี้สามารถสรุปได้ว่าตัวเร่งปฏิกิริยาแพลเลเดียมที่ใช้ควรมีขนาดผลึกของโลหะที่เหมาะสม เพื่อที่จะได้การกระจายตัวของโลหะบนตัวรองรับที่สูง ที่มีการสูญเสียของผลึกโลหะน้อยที่สุด นอกจากนี้ในการศึกษาผลของอุณหภูมิที่ใช้ในการรีดิวซ์ตัวเร่งปฏิกิริยาแพลเลเดียมคลอไรด์บน SiO_2 พบว่าอุณหภูมิการรีดิวซ์ที่เหมาะสมคือ 150 ^{0}C ที่ทำให้ค่าการกระจายตัวของแพลเลเดียมที่วัดโดยวิธีการดูดซับ CO เพิ่มขึ้น ทั้งนี้อาจเนื่องมาจากการสลายตัวของแพลเลเดียมไฮไดรด์เป็นโลหะแพลเลเดียม

ภาควิชา....วิศวกรรมเคมี.....	ลายมือชื่อนิสิต.....
สาขาวิชา....วิศวกรรมเคมี.....	ลายมือชื่ออาจารย์ที่ปรึกษา.....
ปีการศึกษา.....2547.....	ลายมือชื่ออาจารย์ที่ปรึกษาร่วม.....

4670596921 : MAJOR CHEMICAL ENGINEERING
KEYWORDS: LIQUID PHASE HYDROGENATION/ MCM-41/ SILICA SUPPORTED PALLADIUM CATALYST/ 1-HEXENE

ORATHAI TANGJITWATTANAKORN: EFFECT OF PALLADIUM PRECURSORS ON LIQUID PHASE HYDROGENATION OVER SILICA-SUPPORTED PALLADIUM CATALYSTS THESIS ADVISOR: JOONGJAI PANPRANOT Ph.D.,
THESIS CO-ADVISOR: PIYASAN PRASERTHDAM, Dr.Ing. 97 pp. ISBN: 974-53-1767-6

Liquid phase hydrogenation of 1-hexene under mild conditions has been investigated on a series of silica (SiO_2 and MCM-41) supported Pd catalysts prepared from different Pd precursors such as $Pd(NO_3)_2$, $PdCl_2$, and $Pd(OAc)_2$. For both SiO_2 and MCM-41 supports, use of $PdCl_2$ as a Pd precursor resulted in the smallest Pd particle size, the highest Pd dispersion, and consequently the highest hydrogenation activities. Deactivation of the silica supported Pd catalysts in liquid phase hydrogenation was found to be dependent on the palladium particle size. Smaller Pd particles prepared from $PdCl_2$ showed greater metal sintering after 1.5-h batch reaction, whereas leaching of Pd was found to a significant degree for the ones prepared from $Pd(NO_3)_2$ and $Pd(OAc)_2$ (larger Pd particles). An optimum Pd particle size may be needed in order to minimize such loss and enhance Pd dispersion. MCM-41 was partially collapsed during reaction resulting in lower CO chemisorption of the spent Pd/MCM-41 catalyst than that of Pd/SiO_2. The optimum reduction temperature for the $PdCl_2/SiO_2$ was determined to be ca. 150^oC. The results suggest that a complete decomposition of PdH_2 to Pd^0 probably increased the amount of active surface Pd available for the reaction.

Department ……Chemical Engineering…… Student's signature ……
Field of Study……Chemical Engineering…….. Advisor's signature ……
Academic year ……2004…… Co-advisor's signature ……..……

ACKNOWLEDGEMENTS

The author would like to express his sincere gratitude and appreciation to her advisor, Dr. Joongjai Panpranot, for her invaluable suggestions, encouragement during her study, useful discussion throughout this research. Without the continuous guidance and comments from her co-advisor, Professor Piyasan Praserthdam, this work would never have been achieved. I also would like to thank Dr. Aticha Chisuwan Department of Chemistry, Chulalongkorn University, Thailand for the assistance with MCM-41 preparation. In addition, the author would also be grateful to Associate Professor Suttichai Assabumrungrat, as the chairman, and Dr. Seeroong Prichanont, and Dr. Akawat Sirisuk, as the members of the thesis committee. The financial supports of the Thailand Research Fund (TRF), TJTTP-JBIC and Graduate School of Chulalongkorn University are gratefully acknowledged.

Most of all, the author would like to express her highest gratitude to her parents who always pay attention to her all the times for suggestions and listen her complain. The most success of graduation is devoted to my parents.

Finally, the author wishes to thank the members of the Center of Excellence on Catalysis and Catalytic Reaction Engineering, Department of Chemical Engineering, Faculty of Engineering, Chulalongkorn University for friendship and their assistance especially Dr. Okorn Mekasuwandumrong, Mr. Kongkiat Suriye and Miss Vasana Jamsak.

CONTENTS

Page

Page

LIST OF TABLES

LIST OF FIGURES

FIGURE **Page**

FIGURE **Page**

CHAPTER I

INTRODUCTION

Catalytic hydrogenation is one of the most useful, versatile, and environmentally acceptable reaction routes available for organic syntheses. A large number of these reactions are carried out in liquid phase using batch type slurry processes. The types of hydrogenation catalyst finding commercial applications include noble metals, group VIII transition metals, organometallic complexes, and activated alloy catalysts that are either unsupported or supported. The major advantages of noble metal catalysts are their relatively high activity, mild process conditions, easy separation, and better handling properties. Several factors affecting the performance of noble metal catalysts in liquid phase hydrogenation have been extensively investigated. Generally, the factors can be classified into (i) the role of liquid phase composition (substrate structure, solvent effects, etc.), (ii) the effect of catalyst (active sites composition and morphology, support effects, SMSI, modifiers, etc.), and (iii) the effect of reaction conditions (temperature, pressure, etc.) on reaction kinetics.

Palladium is typically the preferred metal for hydrogenation of acetylenes, olefins, carbonyls, aromatic aldehydes and ketones, aromatic and aliphatic nitro compounds, reductive alkylation, hydrogenolysis, and hydrodehalogenation reaction. Common Pd catalyst supports include activated carbon, silica, alumina and to lesser extent, polymer and zeolite. Recently, highly ordered mesoporous materials, such as MCM-41, have been used as supports for metal catalysts and a significant improvement in catalytic activity has been shown. MCM-41 posseses high BET surface area (usually > 1000 m^2/g), uniform pore size with pore dimensions between 1.5-10 nm, and high thermal and hydrothermal stability. The better performances of MCM-41 supported catalysts have been attributed to their high surface areas and superior dispersion of active metals.

The catalytic activity and selectivity of supported Pd catalysts in hydrogenation reaction were often found to be dependent on composition of the palladium precursor used in catalyst preparation. For examples, rates of methanol and methane formation during CO hydrogenation over Pd/CeO_2 catalysts were greater for the catalysts prepared from palladium chloride and palladium acetate than those prepared from palladium nitrate, although the type of Pd precursors did not have a major effect on the selectivities of the products (*W.-J. Shen et al.*, 2000). Mahatal *et al*., (2000), on the other hand, found that $Pd(NH_3)_4Cl_2$ led to lower dispersion of Pd while $Pd(OOCCH_3)_2$ showed good metal dispersion and higher phenol hydrogenation activity for Pd catalysts supported on Al_2O_3 and MgO. Thus, the performances of supported Pd catalysts are dependent not only on the Pd precursors but also the type of metal support used.

Up to date, little is known about the effect of Pd precursor on the characteristics and catalytic activities of Pd catalysts supported on mesoporous materials such as MCM-41 especially in liquid phase hydrogenation. It is the propose of this study to investigate the influence of different Pd precursors on the activity and deactivation SiO_2 and MCM-41-supported Pd catalysts in liquid phase hydrogenation reaction under mild conditions.

CHAPTER II

THEORY

2.1 Hydrogenation Reaction

One of the oldest and most diverse catalytic processes is the selective hydrogenation of functional groups contained in organic molecules to produce (1) fine chemicals, (2) intermediates used in the pharmaceutical industry, (3) monomers for the production of various polymers, and (4) fats and oils for producing edible and nonedible products. Indeed, there are more hydrogenation catalysts available commercially than any other type, and for good reason, because hydrogenation is one of the most useful, versatile, and environmentally acceptable reaction routes available for organic synthesis. With the exception of a few large scales, continuous hydrogenation processes in petroleum refining, hydrogenation products are often made on a small scale in batch reactors. Batch processes are usually most cost effective since the equipment need not to be dedicated to a single reaction. Generally, large stirred autoclave is capable of H_2 pressure up to 140 atm. The catalyst is generally powdered and slurried with reactants; a solvent is usually present to influence product selectivity and to absorb the reaction heat liberated by the reation. Since most hydrogenations are highly exothermic, careful temperature control is required to achieve the desired selectivity and to prevent temperature runaway (Farrauto and Bartholomew, 1997).

2.2 Hydrogenation of Alkenes

The carbon-carbon double bond is in general among the functional groups that are most readily hydrogenated, unless highly substituted and/or strongly hindered. Although the discovery of Sabatier and Senderens in 1897 that ethylene reacted with hydrogen over reduced nickel oxide to give ethane was made at a high temperature in the vapor phase, a large number of alkenes have later been hydrogenated successfully in the liquid phase, frequently under mild conditions using platinum, palladium, and active nickel catalysts such as Raney Ni. However, application of elevated

temperatures and/or pressures is preferred in larger-scale hydrogenations to complete the reaction within a reasonable time using relatively small amounts of catalyst.

The hydrogenation of mono- and disubstituted double bonds is usually rather rapid over most catalysts even under mild conditions. The heat of hydrogenation is also greater for mono- and disubstituted ethylenes than for tri- and tetrasubstitutted ones. Accordingly, care must be taken to prevent the reaction from proceeding too violently with less hindered olefins this can be achieved by adjustion the reaction temperature and the amount of catalyst (Nishimura, 2001).

The generally accepted mechanism for the hydrogenation of double bonds over heterogeneous catalysts was first proposed by Horiuti and Polanyi and was later supported by results of deuteration experiments. It assumes that both hydrogen and alkene are bound to the catalyst surface. The hydrogen molecule undergoes dissociative adsorption [Eq.1], while the alkene adsorbs associative [Eq. 2]. Addition of hydrogen to the double bond occurs in a stepwise manner [Eq. 3 and 4].

While the last step [Eq. 4] is virtually irreversible under hydrogenation conditions, both the adsorption of alkene [Eq. 2] and the formation of alkyl intermediate (half-hydrogenated state) [Eq. 3] are reversible. The reversibility of these steps accounts for the isomerization of alkenes accompanying hydrogenation (Sheldon *et al.*, 2001).

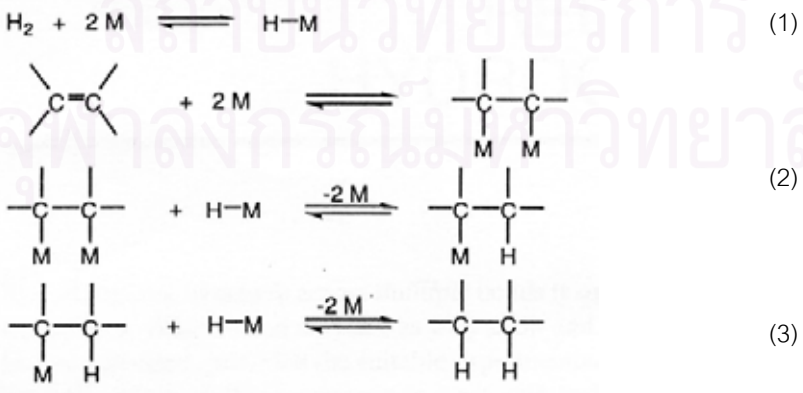

Reaction mechanism for 1-hexene hydrogenation on Pd catalyst is generally proposed as follows:

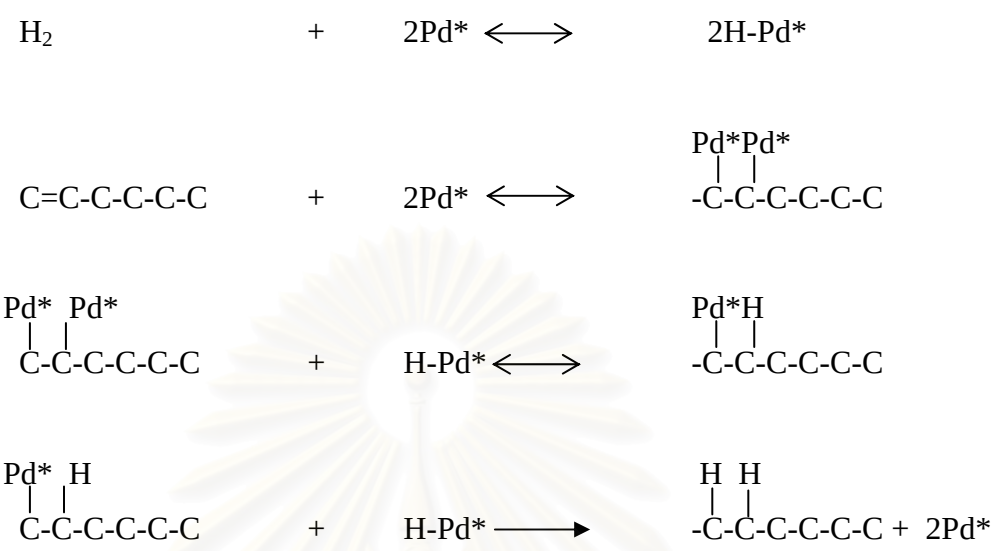

2.3 Hydrogenation Catalysts

The types of hydrogenation catalysts finding commercial applications include noble metals, group VIII transition metals, organometallic complexes, and activated alloy catalysts that are either unsupported or supported. The major advantages of noble metal catalysts are their relatively high activity, mild process conditions, easy separation, and better handling properties. The most commonly used noble metals are Pt, Pd, Rh, and Ru. Generally Pd is more active than Rh or Pt for many hydrogenation reactions on the same carbon carrier (Rylander, 1985a, b). In general, use of a support allows the active component to have a larger exposed surface area, which is particularly important in those cases where a high temperature is required to activate the active component. The supports may be as different as carbon (Rylander, 1979, March, 1985 and Chou, and Vannice, 1987), silica (Frolov *et al.*, 1984 and Cherkashin *et al.*, 1985), alumina (Mathew and Srinivasan, 1995, Weyrich and Holderich, 1997, Kresge *et al.*, 1992 and Beck *et al.*, 1992) and polymer (Corma *et al.*, 1997) in order to obtain higher selectivity and activity. Supported catalysts may be prepared by a variety of methods, depending on the nature of active components as well as the characteristics of carriers for examples, decomposition, impregnation, precipitation, coprecipitation, adsorption, or ion exchange. Both low and high surface area materials are employed as carriers (Nishimura, 2001).

2.4 Ordered Mesoporous Materials

According to the definition of IUPAC, mesoporous materials are those that have pore diameters between 20 and 500 Å. Examples of mesoporous solids include silica gel (Iler, 1979) and modified layered materials (Landis and Aufdembrink, 1991), but the pores in these materials are irregularly spaced and usually have a wide distribution of pore sizes. A considerable synthetic effort has been devoted to developing highly uniform frameworks with pore diameters within the mesoporous range. The structure of this mesoporous silicate and aluminosilicate family that has received the most attention is referred to as MCM-41, which consists of uniform cylindrical pores arranged in a hexagonal array. The pore dimensions can be tailored in the range of 1.5-10 nm depending on synthesis chemicals and conditions. The BET surface area is usually greater than 1000 m^2 /g with high sorption capacities of 0.7 ml/g.

The MCM-41 mesoporous structure formation of silica is base upon biomineralization and biomimetic chemistry in which organic and inorganic species interact and self-assemble into nanosize structures. A typical synthesis starts from preparation of an aqueous surfactant solution. A silica source, combined with an acid or base liquid catalyst to aid in the polymerization of the silica, is then added to the aqueous surfactant solution, and the slurry is stirred. This room temperature mixing of the reactants allows the hydrophilic heads of the surfactant to interact with the silica in solution by electrostatically attracting silica molecules to the micelle surface. The solution is then heated under autogeneous pressure at temperatures of 100-200 °C for 24 to 48 hours. At these elevated temperatures, the silica extensively polymerizes and condensed around the micelles. The interaction of the inorganic and organic phases is believed to align the micelles via a self-assembly mechanism to form the as-synthesized mesostructured composite. Subsequent removal of the organic surfactant by calcination in air or by solvent extraction creates the highly ordered mesoporous structure. Beck *et al.* proposed two possible mechanistic pathways for MCM-41 formation: (1) a liquid crystal templating mechanism, where the MCM-41 structure is formed around micelles existing as single cylindrical aggregates; (2) a mechanism where the addition of the silicate results in the ordering of the subsequent silicate-

encaged surfactant micelles. A schematic of this formation mechanism is shown in Figure 2.1.

The synthesis of these mesoporous materials has been found to be a strong function of several variables in the system (Corma, 1997; Kruk *et al.*, 1999; Carrott *et al.*, 1999; Chen *et al.*, 1997; Liepold *et al.*, 1996; Kruk *et al.*, 2000). The surfactant-to-silica ratio in the synthesis mixture has been identified as capable of determining the type of mesoporous structrue formed. Typically, this molar ratio is less than or equal to 0.5 for MCM-41 formation. At values greater than 0.5, other mesostructures i.e., cubic symmetry MCM-48 and Lamellar symmetry MCM-50, have been reported. The basicity, temperature, and time also determine the rate of polymerization of the silica precursor.

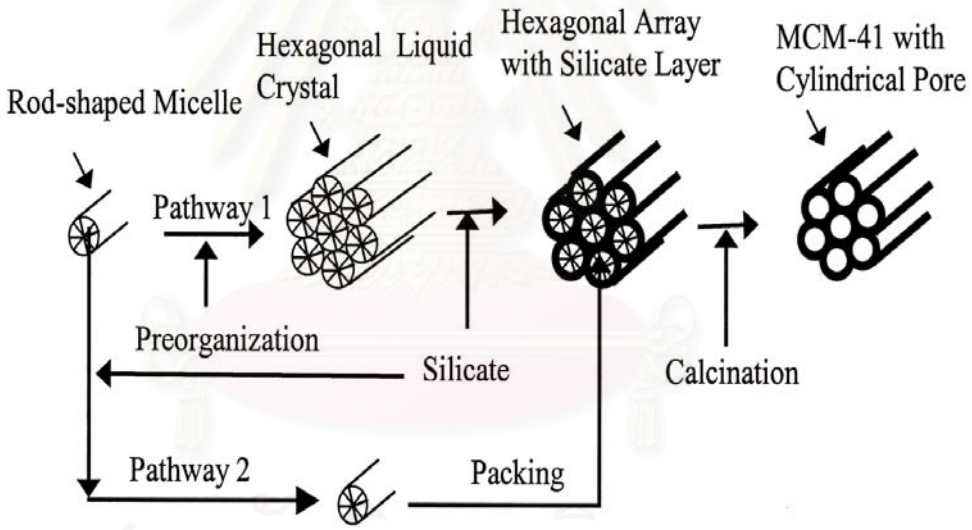

Figure 2.1 Possible mechanistic pathways for the formation of MCM-41: (1) liquid-crystal initiate and (2) silicate anion initiate

CHAPTER III

LITERATURE REVIEWS

Liquid phase hydrogenation of alkene on supported Pd catalysts has been extensively studies. Many factors affecting the catalyst performances catalyst such as effects of reaction condition and solvent, support and preparation condition and type of catalyst were reported. Following are reviews of some recent studies on such topics.

3.1 Effect of reaction condition and solvent

Istvan Palinko (1995) studied hydrogenation of 1-hexene and cyclohexene over silica-supported Pt, Pd and Rh catalysts in the liquid phase, in the presence of quinoline or carbon tetrachloride at room temperature. The catalysts were prepared using either impregnation or ion-exchange methods. They reported that the hydrogenation was a zero-order reaction and carbon tetrachloride strongly influences the hydrogenation of 1-hexene over Rh/SiO_2 and Pd/SiO_2 catalysts. Deactivation of 1-hexene hydrogenation upon the adsorption of either additive seemed to be structure sensitive over Pd/SiO_2 catalysts. But this was not the case for hydrogenation of cyclohexene.

S. David Jackson and Lindsay A. Shaw (1996) studied the competitive hydrogenation of phenyl acetylene and styrene over a palladium/carbon catalyst. They found that the order in phenyl acetylene changed from zero order to first order at approximately 60% conversion. This behavior was ascribed to catalyst surface being unable to saturate with the hydrocarbon due to low concentration in solution.

M.A. Armendia *et al.* (1997) studied the hydrogenation of citral with Pd catalysts supported on mixed 80:20 $SiO_2/AlPO_4$ and sepiolite from Vallecas (Madrid, Spain). They investigated the influence of reaction variables such as temperature, hydrogen pressure and the type of solvent in order to optimize the reduction process. .

The solvent has a marked effect on the reduction rate; thus, nonpolar solvents lead to greater reduction rates. They found that the presence of additives of Lewis acid type such as $FeCl_2$ increases the selectivity towards geraniol and nerol.

Z. Dobrovolna *et al.* (1998) studied competitive hydrogenation of alkene, alkyne and diene substrates (C_6- C_8) over palladium and platinum catalysts at 20 °C and atmospheric pressure. They found that hydrogenation of alkynic and dienic substrates were preferred in alkyne-alkene and diene-alkene systems, respectively. In these systems, palladium catalyst selectivity was higher than that of the platinum catalyst due to higher relative adsorption coefficients for corresponding substrate couple on the palladium catalyst.

T. Nozoe *et al.* (2001) investigated the non-solvent hydrogenation of solid alkynes and alkenes using supported palladium catalysts. Trans-Stilbene and carboxylic acids with α,β-C=C bonds were employed as the alkene-type substrates for the non-solvent hydrogenation. Their hydrogenation proceeded over a Pd/SiO_2 catalyst at room temperature in a hydrogen stream. The hydrogenation rate of the trans-stilbene under the non-solvent conditions was lower than the hydrogenation in tetrahydrofuran (THF). The non-solvent hydrogenation of the C=C bond in diphenylacetylene or phenylpropiolic acid proceeded over a Pd/C catalyst more smoothly than their hydrogenation in THF.

3.2 Effect of catalyst support

Dario Duca *et al.* (1995) studied the liquid phase, selective hydrogenation of phenylacetylene on pumice-supported palladium catalysts for a large range of metallic dispersions ($14\% \leq D_x \leq 62\%$). The powder used as support for their catalysts was a waste product from the production of Pumex Spa-Lipari, with a particle size smaller than 45 μm. Activity and selectivity data were reported and compared with other supported palladium catalysts. They suggested that Pd/pumice catalysts could be interesting for industrial application because of their high activity and selectivity at high metal dispersions.

Z.M. Michalska *et al.* (1998) studied the catalytic behavior of palladium supported on polyamides having a pyridine moiety in the liquid phase hydrogenation of alkadienes and alkynes at 25 °C and 1 atm pressure. The polymer supported palladium catalyst demonstrated high activity for alkyne hydrogenation. Such a different in selectivity was ascribed to the strong metal-support interaction that exists between palladium and the polymer functionalities. The results indicated that the rate of hydrogenation was affected more by the solvent polarity than by the solubility of hydrogen in the solvent. The stability and very good recycling efficiency of these catalysts made them useful for prolonged use.

S. David Jackson *et al.* (1999) studied the hydrogenation of cyclopentene, cyclohexene, cycloheptene, and cis-cyclooctene over Pd/alumina, Pd/carbon, Pd/silica, and Pd/zirconia catalysts. The hydrogenation reaction and the carbon deposition reaction both showed evidence for particle size sensitivity and the trend in activity with particle size was not the same for all the cycloalkenes, with cycloheptene hydrogenation increasing with particle size. This behaviour can principally be related to the strength and mode of adsorption of the cycloalkene, although the adsorbed state of hydrogen may also influence reactivity.

B.M. Choudary *et al.* (1999) compared Pd catalysts supported on mesoporous materials, Pd/Si-K10 and Pd/MCM-41, with a microporous Pd/Y-zeolite. Catalysts were prepared by ion exchange method and their catalytic properties for the hydrogenation of alkenes, alkynes and semi-hydrogenation of alkynes were investigated. Pd/MCM-41 was about two times more active than Pd/Si-K10. Pd is not well dispersed on any of the three supports when the catalyst was prepared in organic media. It is known that selectivity decreases for semi-hydrogenation when dispersion increases, so that this poor dispersion is acceptable. All catalysts were active in the hydrogenation of alkynes giving high yields of alkenes but Pd/MCM-41 showed highest activity. In conclusion, mesoporous supports give satisfactory results for the semi-hydrogenation of acetylenic compound in fine chemistry.

S. Shimazu *et al.* (2002) studied the synthesis and the characterization of the palladium complexes grafted on MCM-41 mesopore surface via silane coupling ligands (AEAPSi) and their catalytic behavior for the hydrogenation of dienes

with/within a hydroxyl group. The MCM-41 supported catalyst had a large amount of the unmodified-OH groups in th mesopore as well as the AEAPSi functional group. The MCM-41 supported catalyst exhibited high activity and high regioselectivity in the hydrogenation of dienes with -OH group.

S. Albertazzi *et al.* (2003) studied the behavior of different catalysts containing 1 wt. % of noble-metal inside a mesoporous MCM-41 in the hydrogenation of naphthalene. Only the Rh- and Pd-containing catalysts were active in the test performed at atmospheric pressure. Performing the tests under pressure (6.0 MPa) the catalytic activity grew significantly, evidencing the following scale of activity for the noble-metals investigated: Pt>Rh>>Pd>>>>Ru≈Ir, with the latter two catalysts that deactivated in the 1 h of time on steam.

3.3 Effect of catalyst preparation condition and type of catalyst

U. K. Singh and M. Vannice (2001) studied liquid-phase citral hydrogenation over SiO_2-supported Group VIII metals at 300 K and 1 atm. The catalysts were prepared using an incipient wetness technique. The initial TOF (turnover frequency) for citral hydrogenation varied by three orders of magnitude and exhibited the following trend: Pd>Pt>Ir>Os>Ru>Rh>Ni>Co>>Fe (no activity was detected over $FeSiO_2$). With the exception of Ni/SiO_2, all catalysts exhibited substantial deactivation due to citral and/or unsaturated alcohol decomposition to yield adsorbed CO that poisoned active sites responsible for hydrogenation.

S. Tanaka *et al.* (2002) prepared Pd/SiO_2 catalysts by a complexing agent-assisted sol-gel method and impregnation methods using an organic complexing agent (imp-org) or water (imp-w) as the impregnation solvent. The Pd/SiO_2 were characterized by TG-DTA, FT-IRs, C NMR, XRD, TEM, XPS, and CO adsorption, and the difference between the preparation methods was discussed. They found that the palladium particles in the sol-gel catalysts were much smaller and more uniform in size than those in the corresponding impregnation catalysts. The CO adsorptions for both impregnation catalysts decrease with the activation temperature after showing the maxima.

R.A.W. Johnstone *et al.* (2003) studied hydrogenation of alkenes over palladium and platinum metals supported on a variety of metal (IV) phosphates. Platinum and palladium catalysts were prepared by first exchanging the acidic protons followed by their reduction to metal. They found that rate of hydrogenation of 1-octene and 4-methylcyclohexene over a series of platinized and palladized metal (IV) phosphates, some of which were more effective than standard Pd/C catalyst. The variation may correlate with surface topography but does not appear to correlate within the electronegativity of the metal in the metal phosphate.

O. Dominguez-Quintero *et al.* (2003) investigated palladium nanoparticle in the hydrogenation catalysis of different substrates (1-hexene, cyclohexene, benzene, 2-hexanone and benzonitrile). Palladium nanoparticles (1.9 nm.) stabilized was obtained from the reduction of organometallic precursor (palladium (II) bis-dibencylidene acetone) with hydrogen. The highest hydrogenation rate was found with 1-hexene with a TOF of 38,250 mole of product/ (mole of metal/h) at 25°C and 30 psi pressure. They presented that the catalytic potential of the Pd/SiO_2 systhesized by an organometallic route renders an extremely active nanomaterial which shows little aggregation after catalytic reactions even at 145 °C.

Generally, the activity and selectivity of the catalysts for hydrogenation reaction depend on metal dispersion and metal particle size. Changing metal precursors and/or reduction temperature can result in different metal particle size. Following are reviews of recent studies on the effects of reduction temperature and Pd precursors in hydrogenation reaction.

3.4 Effect of reduction temperature

D.C. Koningsberger *et al.* (1995) studied the structure of the metal particles and the metal-support interface of a $Pt/\gamma\text{-}Al_2O_3$ catalyst was determined by EXAFS after low temperature reduction (LTR: 300°C) and high temperature reduction (HTR:450°C). The clusters have excellent thermal stability as the particle size remains 12 atoms per cluster upon increasing the reduction temperature from 300°C to 450°C. However, the structure of the metal-support interface is a strong function

of the reduction temperature. The results show that the influence of the reduction temperature on the structure of the metal-support interface of platinum particles on a amorphous support is similar to platinum particles which reside in cavities of zeolites.

C.A. Koh *et al.* (1997) studied the structure of MCM-41 material during heat treatment (calcination) and determined catalytic performance of a series of Pd/MCM-41 catalysts, prepared by an incipient wetness technique, for selective hydrogenation of 1-hexene and benzene. Their temperature-programmed reduction (TPR) measurements for the calcined Pd catalyst series showed that about 70% of the PdO contained in the catalysts were reduced at sub-ambient temperature and the other 30% of PdO were reduced within 298-323 K (G.C. Bond, private communication), while the pure MCM-41 showed no reduction up to 873 K. TEM results showed that the Pd metal particles in the reduced Pd/MCM-41 catalysts were located in the pores of MCM-41 with good distribution.

Wen-Jie Shen *et al.* (2001) studied the effect of the temperature of reduction on the activity and selectivity of a Pd-CeO_2 catalyst was studied for the hydrogenation of CO and CO_2. A drastic decrease in the overall conversions of carbon oxides and a significant modification in the product selectivity were observed when the catalyst was reduced at 773 K. The main reason for the decrease in the overall catalytic activity was the occurrence of severe sintering of palladium particles during high temperature reduction, evidenced by extended X-ray absorption fine structure (EXAFS) and X-ray diffraction (XRD) measurements. The remarkable changes in the selectivities of the products were explained by the decoration phenomenon of palladium surface by reduced ceria species due to the phase change between CeO_2 and Ce_2O_3 upon reduction at 773 K.

Esa Toukoniitty *et al.* (2001) studied the effect catalyst reduction temperature in enantioselective hydrogenation of 1-phenyl-1,2-propanedione over commercial Pt/Al_2O_3 catalyst. Effect of catalyst reduction temperature was studied at three different temperatures (170, 400 and 455°C). Highest reaction rates and enantiomeric excesses were obtained with the catalyst reduced at 400°C. Methane was desorbed from the catalyst at temperatures between 263 and 383°C which could be the explanation for the lower activity of the catalyst reduced at 170°C. It was

demonstrated that catalyst reduction temperature plays an important role in obtaining high enantiomeric excesses.

D. J. Duvenhage and N. J. Coville (2002) studied the effect of reduction temperature on the performance (activity and selectivity) of a Fe:Co/TiO_2 catalyst the Fischer–Tropsch reaction has been investigated. Various techniques (CO chemisorption, TPO, TPR, DSC, BET and Mössbauer Spectroscopy) have been utilized to relate the performance of the above catalyst system. Catalyst reduction temperature increased the surface atom ratio, degree of reduction and CO chemisorption, and hence the active metal dispersion, and overall catalytic behaviour.

Wolfgang Reichl and Konrad Hayek (2002) studied vanadia adlayers on a Rh surface promote the hydrogenation of CO. The reaction rate is always increased with respect to the bare Rh surface but depends strongly on the reduction temperature. After reduction up to 673 K the observed rate increase can be correlated to the existence of two VO_x adlayer phases of different oxygen content. Enhanced CO dissociation at the perimeter sites of the VO_x islands leads to enhanced initial hydrogenation rates but also to enhanced deactivation of the catalyst. Raising the reduction temperature above 773 K results in the formation of metallic V, which is partially dissolved in the bulk, resulting in a V/Rh subsurface alloy with a Rh-terminated surface. This surface is particularly active for CO hydrogenation and less susceptible to deactivation by carbon deposition.

G.Lafaye *et al.* (2003) studied two series of alumina supported Rh-Ge catalysts. They were characterized by temperature-programmed reduction (TPR) and by their activity for the liquid phase hydrogenation of citral used as model reaction. The citral conversion and the selectivity to unsaturated alcohols increase with the germanium content and go through a maximum as a function of the reduction temperature of catalysts. For reduction temperatures in the 150–350 °C range, bimetallic catalysts exhibit better hydrogenating properties in the solvent isopropanol in comparison with n-heptane while the reverse occurs after a reduction at 500 °C.

3.5 Effect of palladium precursor

M. Schneider *et al.* (1994) synthesized mesoporous to macroporous palladium-titania aerogels with high surface by the sol-gel-aerogel route. Both the palladium particles and the titania matrix possess a remarkable structural stability up to 773 K. By varying the Pd precursor solution, different palladium particle size distributions can be obtained. The catalytic studies showed that the activities were much higher for the hydrogenation of trans-stilbene than those for the benzophenone. The hightest dispersed palladium-titania aerogels, derived from $Pd(OAc)_2$, showed superior activity and selectivity for 4-methylbenzaldehyde hydrogenation compared to impregnated titania-supported Pd catalyst.

Ali and Goodwin (1998) studied two different precursors [$PdCl_2$ and $Pd(NO_3)_2$] and three supports [SiO_2, Al_2O_3 , and SiO_2–Al_2O_3] in CO hydrogenation were investigated. The dispersion of the Pd particles on the prepared catalysts, as evaluated by CO chemisorption, was not affected by either the Pd precursor or the support used. However, the catalysts prepared using $PdCl_2$ showed higher overall activities than those prepared using $Pd(NO_3)_2$ for a given support.

Nagendranath Mahata1 and V. Vishwanathan (2000) studied the influence of palladium precursors on structural properties and phenol hydrogenation characteristics of Al_2O_3- and MgO-supported palladium catalysts. $Pd(OOCCH_3)_2$ shows good metal dispersion and phenol hydrogenation activity $Pd(NH_3)_4Cl_2$ leads to lower dispersion of Pd, probably due to the presence of inherent NH_3 (a reducing agent) and facile surface mobility of the precursor. The initial activity of phenol hydrogenation is directly proportional to the palladium area over the catalysts prepared with $Pd(OOCCH_3)_2$ and $Pd(NH_3)_4Cl_2$; the activity shows a negative deviation over the catalysts originating from $PdCl_2$. Palladium precursors do not have a significant influence on the distribution of products.

W.-J. Shen *et al.* (2001) studied catalytic behavior of Pd/CeO_2 catalysts in methanol synthesis through hydrogenation of carbon monoxide. Catalysts prepared from palladium chloride and palladium acetate showed much higher overall catalytic activities than those prepared using palladium nitrate. Palladium precursors did not

have a significant influence on the distribution of products, very similar selectivities of methanol and methane were obtained. The palladium precursor, or more specifically its anion, had an effect on the final palladium particles, and therefore affected the interaction between Pd and ceria, which would cause different reaction results.

D. Nazimek and W. Cwikła-Bundyra (2004) studied catalytic reduction of NO to nitrogen was carried out over supported platinum and palladium catalysts that were derived from chlorides and nitrates as the precursors. The activity was largely dependent not only on the kind of metal support used but also on the precursors. The Pd supported catalyst derived from $Pd(NO_3)_2$ was much more active within 773K temperature than the catalyst prepared from $PdCl_2$. The highest activity was revealed by the Pd/Al_2O_3 obtained from nitrates.

From the literature review, different conclusions have been drawn in terms of activity and selectivity. For some reactions catalysts prepared using $PdCl_2$ showed higher activity than those prepared using $Pd(NO_3)_2$ but for some cases opposite trend was found. The activity and the selectivity are, therefore, dependent not only on the kind of Pd precursors used but also on the catalyst support and type of reaction studied as well.

3.4 Catalyst Deactivation in Liquid Phase Reaction

Study of catalyst deactivation in liquid phase reaction studies is somewhat difficult because of the high number of factors potentially involved such as sintering and leaching of active components, poisoning of active sites by heteroatom-containing molecules, inactive metal or metal oxide deposition, impurities in solvents and reagents, and oligomeric or polymeric by-products. Because of many factors involved in activity and selectivity decay and non-identical catalysts for different lots, there is a high probability of irreproducible results (Michele Besson and Pierre Gallaezot, 2003). In this work, the main causes of deactivation in liquid phase reaction such as metal sintering and metal leaching were focused.

Fengyu Zhao *et al.* (2000) studied the details of this mass transfer between solvent and support by using homogeneous or heterogeneous catalysts in the absence or presence of additional palladium-free support materials. The results showed that Pd exists in solution, on the support, and in the form of free colloidal particles during and after the Heck reaction and the transfer of Pd between these phases depends on the surface nature of the supports and reaction conditions used.

Peter Albers *et al.* (2001) studied the major causes for deactivation such as particle growth for, coke deposition, and leaching. They found that the leaching of precious metal can be minimized by either improving the availability of hydrogen in the liquid reaction medium or by optimizing the "catalyst side" of the process. In term of modifying the "catalyst side" of the process two approaches are proposed (1) to use of smaller quantities of catalyst for reaction and or (2) decrease the precious metal loading of the catalyst. Unfavorable and undesired effect about sintering and agglomeration may be suppressed by means of adequate impregnation agents and procedures, controlled temperature, and use of suitable support materials (R.J. Card, *et al.*, 1983)

Roland G. Heidenreich *et al.* (2002) studied parameter that influence the palladium leaching during and after Heck reactions of aryl bromides with olefins catalyzed by heterogeoeous Pd on activated carbon systems. The results showed that the Pd concentration in solution correlated with the nature of the starting materials and products, the temperature, the solvent, the base and the atmosphere (argon or air). Lower temperatures, higher concentrations and stronger interactions of the bromoarenes with Pd^0 clearly increase Pd leaching.

Michele Besson and Pierre Gallezot (2003) reviewed the factors contributing to the deactivation of metal catalysts employed in liquid phase reactions for the synthesis of fine or intermediate chemicals. The main causes of catalyst deactivation are particle sintering, metal and support leaching, deposition of inactive metal layers or polymeric species, and poisoning by strongly adsorbed species. Leaching of metal atoms depends upon the reaction medium (pH, oxidation potential, chelating properties of molecules) and upon bulk and surface metal properties.

Joongjai Panpranot *et al.,* (2004) investigated and compared the characteristics and catalytic properties of Pd/MCM-41 and Pd/SiO_2 catalysts in terms of Pd dispersion, catalytic activities for liquid-phase hydrogenation of 1-hexene, and deactivation of the catalysts. High Pd dispersion was observed on Pd/MCM-41-large pore catalyst while the other catalysts showed relatively low Pd dispersion due to significant amount of Pd being located out of the pores of the supports. Based on CO chemisorption results, the catalyst activities seemed to be primarily related to the Pd dispersion and not to diffusion limitation since TOFs were nearly identical for all the catalysts used in this study. In all cases, leaching and sintering of Pd caused catalyst deactivation after 5-h batch reaction. However, compared to Pd/SiO_2 with a similar pore size, Pd/MCM-41 exhibited higher hydrogenation activity and lower amount of metal loss.

CHAPTER IV

EXPERIMENTAL

4.1 Catalyst Preparation.

4.1.1 Synthesis of MCM-41

Pure silica MCM-41 with 3 nm pore diameter was prepared in the same manner as that of Cho et al. (D.H.Cho *et al.*) using the gel composition of CTABr: 0.3 NH_3: 4 SiO_2: Na_2O: 200 H_2O, where CTABr denotes cetyltrimethyl ammonium bromide. Briefly, 20.03 g of colloidal silica Ludox AS 40% (Aldrich) was mixed with 22.67 g of 11.78% sodium hydroxide solution. Another mixture comprised of 12.15 g of CTABr (Aldrich) in 36.45 g of deionized water, and 0.4 g of an aqueous solution of 25% NH_3. Both of these mixtures were transferred into a Teflon lined autoclave, stirred for 30 min, then heated statically at 100^{o}C for 5 days, the pH of the gel was adjusted to 10.2 using 30% acetic acid every 24 h. The obtained solid material was filtered, washed with water until no base and dried at 100^{o}C. The sample was then calcined in flowing nitrogen up to 550^{o}C (1-2 ^{o}C/min), then in air at the same temperature for 5 hours, and is referred to in this work as small pore MCM-41. The chemicals used in synthesis of MCM-41 are shown in Table 4.1

Table 4.1 Chemicals used in the synthesis of MCM-41

Chemical	Supplier
cetyltrimethyl ammonium bromide	Aldrich
colloidal silica Ludox AS 40%	Aldrich
aqueous solution of 25% NH_3	BDH
30% acetic acid	Carlo Erba

4.1.2 Preparation of small pore silica

Small pore silica was chromatographic grade silica gel (SiO_2) granulars 100-200 mesh obtained commercially from Grace Davision Co.,Ltd. (USA).

The silica support particles were calcined at 550°C for 8 h. in a furnace to eliminate adsorbed water and other impurities. The temperature of furnace was increased from ambient temperature to 550°C at the heating rate 2°C/min. The calcined silica was removed from the furnace, cooled down to room temperature and stored in a desiccator.

Silica	Supplier
MCM-41	Synthesis in our laboratory
Small pore silica	Grace Davison Co.,Ltd. (USA)

4.1.3 Palladium Loading

The palladium loading procedures are as follows:

1. The previously calcined different silica supports were impregnated with an aqueous solution of palladium by the incipient wetness technique. The type of solvent that using preparation an aqueous solution of palladium are shown in Table 4.2 Using the water capacity measurement obtained previously for the silica particles, a sufficient amount of the palladium precursor was added to obtain a 0.5% by weight of palladium.
2. After an impregnation, the catalysts were dried at 110°C for 16 h.
3. The dried catalysts were calcined at 500°C for 2 hours in a furnace.
4. Finally, the catalysts were cooled down and stored in desiccators.

Table 4.2 The types of palladium precursor

Palladium precursor	Solvent
Palladium(II)acetate (Aldrich)	Acetone
Palladium nitrate dihydrate (Aldrich)	Water
Palladium(II)chloride (Aldrich)	HCl 37%: water (1:1); heat up 80 ^{0}C

.

4.2 The Reaction Study in Liquid Phase Hydrogenation

4.2.1 Chemicals and Reagents

The chemicals and reagents used in the reactions are shown in Table.4.3

Table 4.3 The chemicals and reagents used in the reaction

The chemicals and reagents	Supplier
High purity grade Hydrogen (99.99vol. %)	Thai Industrial Gases Limited
High purity grade Nitrogen (99.99vol. %)	Thai Industrial Gases Limited
Absolute ethyl alcohol (99.99vol. %)	Mallinckrodt
1-Hexene purum (96vol. %)	Fluka

4.2.2 Instruments and Apparatus

The schematic diagram of the liquid phase hydrogenation reaction of 1-hexene is shown in Figure 4.1 The part of instruments and apparatus are illustrated and explained as follows:

The Autoclave reactor

The autoclave (Tiatsu Co.,Ltd. Japan) has size 100 ml and 4 cm inside diameter, which is made from stainless steel. It consists of three paths, which are used to feed gas (nitrogen or hydrogen) and reactant and vent gas. Hot plate stirrer is used to stir by magnetic stirrer and heat up (detect temperature by thermometer). This autoclave can be operated at moderate temperature (0-200°C) and pressure (0-10 MPa).

Gas controlling system

Nitrogen cylinder is equipped with a pressure regulator (0-2000 psi). Hydrogen gas is allowed to flow into autoclave by using a pressure regulator (0-350 psi). A needle valve is used to release gas from the autoclave. A ball valve is used to feed reactant flow into autoclave.

Gas chromatograph

A gas chromatograph (Shimadzu GC-9A) equipped with a flame ionization detector (FID) was used to analyzed liquid feed and product. The operating conditions for GC and detector are shown in Table 4.4

Table 4.4 Operating conditions for the gas chromatograph

Gas Chromatograph	Shimadzu GC-14A
Detector	FID
Packed column	Chemical C 18 80/100 8ft
Carrier gas	Nitrogen (99.99vol. %)
Flow rate of carrier gas	25 cc/min
Column temperature	50°C
Detector temperature	200°C
Injector temperature	200°C

4.2.3 Hydrogenation procedure

The hydrogenation procedures are explained in the details below that consist of 2 steps of reaction.

Reduction step

Approximately 0.1 gram of supported Pd catalyst was placed into the autoclave. The system was purged with nitrogen to remove remaining air. Next, hydrogen was switch at a volumetric flow rate of 100 ml/min to reduce supported Pd catalyst at room temperature for 2 h.

Reactant preparation and hydrogenation step

1 ml of 1-hexene and 7 ml of ethyl alcohol were mixed in a beaker, and then set in the 100 ml feed column. Next, the reaction mixture was introduced into the reactor with nitrogen. Afterwards, hydrogen was purged to remove remained nitrogen and keep for the

reaction. The liquid phase hydrogenation reactions were carried out at room temperature and 1 atm and started the reaction with a stirring magnetic stirrer. The content of hydrogen consumption was monitoring every five minutes by noting the change in pressure of hydrogen for 1.5 hour. The products were determined by a gas chromatograph.

4.3 Catalyst Characterization

4.3.1 Atomic absorption spectroscopy

The bulk composition of palladium was determined using a Varian Spectra A800 atomic adsorption spectrometer at the Department of science service Ministry of science technology and environment.

4.3.2 N_2 physisorption

The BET surface areas pore volumes, average pore diameters, and pore size distributions of the catalysts were determined by N_2 physisorption using a Micromeritics ASAP 2000 automated system. Each sample was degassed in the Micromeritics ASAP 2000 at 200^{o}C for 4 hours prior to N_2 physisorption.

4.3.3 X-ray diffraction (XRD)

The XRD spectra of the catalysts was measured using a SIEMENS D5000 X-ray diffractometer and Cu Kα radiation with a Ni filter in the 2-10^{o} or 20-80^{o} 2θ angular regions. The crystallite size was calculated from the Scherrer equation. The value of shape factor, K, was taken to be 0.9.

4.3.4 Scanning electron microscopy (SEM)

Catalyst granule morphology was obtained using a JEOL JSM-35CF scanning electron microscope operated at 20 kV at the Scientific and Technological Research Equipment Center, Chulalongkorn University (STREC).

4.3.5 Transmission electron microscopy (TEM)

Sample of catalysts for TEM were loaded into volatile liquid (ethanol) and then, a suspension in volatile liquid was prepared from the sample powder, often assisted by Ultrasonic agitation for ten minutes. Next, this suspension was dropped on to thin Formvar supported on copper grids and dry. The palladium oxide particle size and distribution of palladium were observed using a JEOL-TEM 200CX transmission electron microscope operated at 100 kV at the Scientific and Technological Research Equipment Center, Chulalongkorn University (STREC)

4.3.6 CO-pulse chemisorption

Relative percentages of palladium dispersion were determined by pulsing carbon monoxide over the reduced catalyst. Approximately 0.2 g of catalyst was placed in a quartz tube, incorporated in a temperature-controlled oven and connected to a thermal conductivity detector (TCD). Prior to chemisorption, the catalyst was reduced in a flow of hydrogen (30cc/min) at room temperature for 2 h. Then the sample was purged with helium for 1 h. Carbon monoxide was pulsed at room temperature over the reduced catalyst until the TCD signal from the pulse was constant.

4.3.7 Temperature programmed reduction (TPR)

TPR was used to determine the reducibility of catalysts. The catalyst sample of ca. 200 mg and temperature ramping from 35^{o}C to 300^{o}C at 10^{o}C/min were used in the operation. The carrier gas was 5 %H_2 in argon. During reduction, a cold trap was placed

before the detector in order to remove water produced. A thermal conductivity detector (TCD) was used to measure the amount of hydrogen consumption.

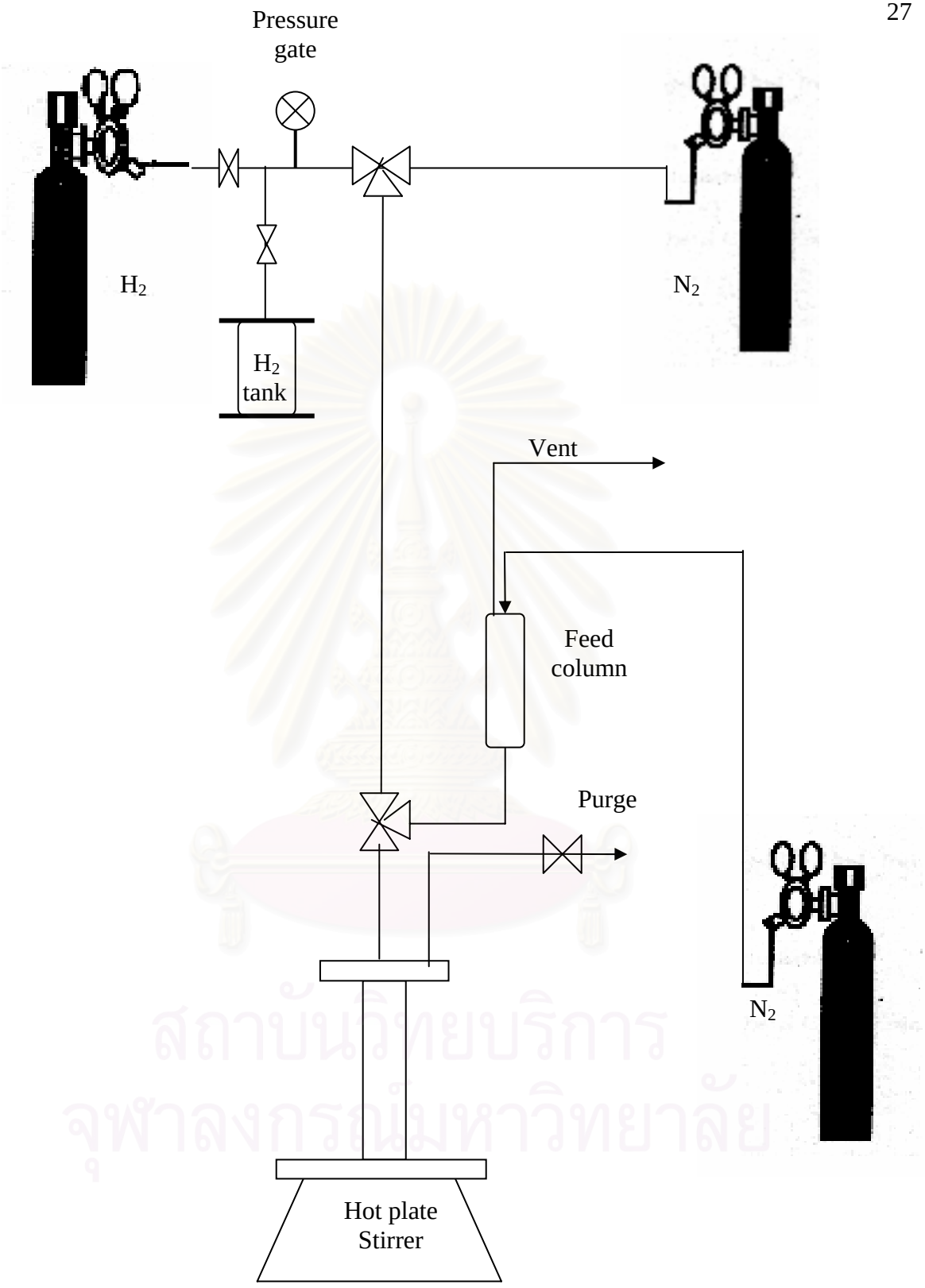

Figure 4.1 A sahematic of liquid phase hydrogenation system

CHAPTER V

RESULTS AND DISCUSSION

Supported metal catalysts are usually prepared by impregnation of a support with an aqueous solution containing desired amount of metal salts. In this chapter, the effect of palladium precursors used for preparation of SiO_2 and MCM-41 supported Pd catalysts on the dispersion of palladium was investigated. The catalytic activities of these catalysts were tested for liquid phase hydrogenation of 1-hexene at 30°C and 1 atm. The characteristics of the catalysts before and after reaction were also discussed in this chapter. The catalysts before performing reaction test are called fresh catalysts and the catalysts after used are called spent catalysts. The results and discussion are divided into three parts. The first part (section 5.1) shows kinetic study of liquid phase hydrogenation of 1-hexene over supported Pd catalysts**.** The second part (section 5.2) demonstrates the characteristics of the catalysts obtained from various analysis techniques such as N_2 physisorption, X-ray diffraction, scanning electron microscopy, transmission electron microscopy, atomic adsorption spectroscopy, CO-pulse chemisorption, and temperature programmed reduction. And the last section (section 5.3) is the study of the effect of reduction temperature on the CO chemisorption activity of the catalysts.

5.1 Liquid Phase Hydrogenation of 1-Hexene over Various SiO_2- and MCM-41-Supported Pd Catalysts

Liquid-phase hydrogenation of 1-hexene under mild conditions was carried out as a model reaction to compare the hydrogenation activity of all the catalysts. The effects of external and internal mass transfer on reaction rate were studied by varying the speed of stirrer and using different particle sizes of palladium catalysts, respectively. In all cases, the same amount of catalyst of approximately 0.1 gram was used.

5.1.1 Effect of Mass Transfer

Figure 5.1 shows the relationship between rate of reaction and stirrer speed. The rates of reaction were found to be constant for all speeds of the stirrer used. This suggests that external mass transfer has no effect on the reaction rate. Figure 5.2 shows a plot between rate of reaction and particle size of supported palladium catalysts. It was also found that there was no significant internal mass transfer limitation (pore diffusion effects) on the reaction rate. Thus, the kinetics of the reaction was mainly controlled by the reaction on the catalyst surface (in this case Pd metal).

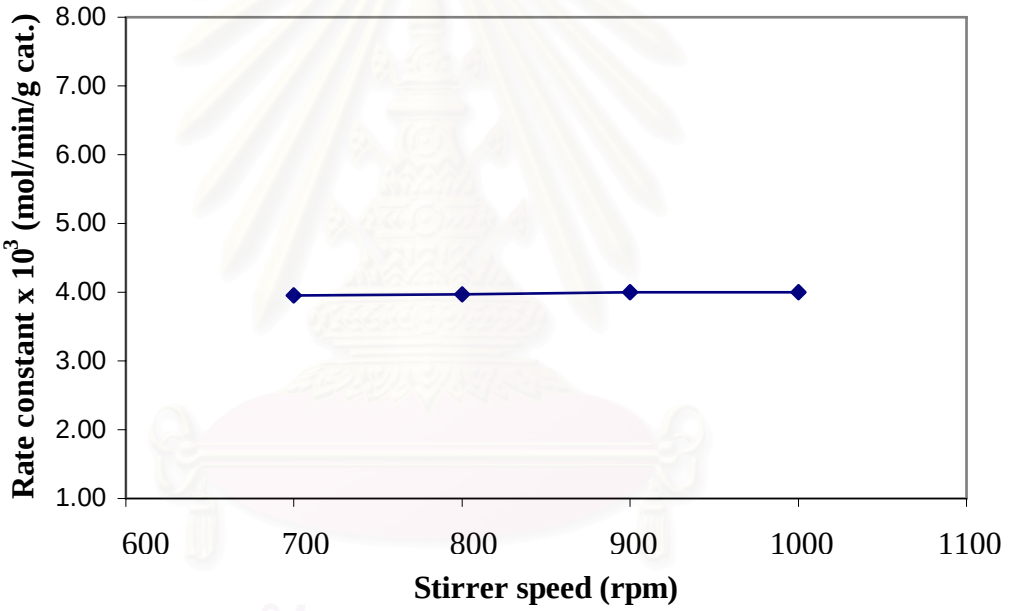

Figure 5.1 Plot of rate constant of $Pd(NO_3)_2$/MCM-41 catalysts for liquid phase hydrogenation of 1-hexene vs. speed of mixing (Reaction conditions were 30^{o}C, 1 atm. and 1-hexene/ethanol = 1:7)

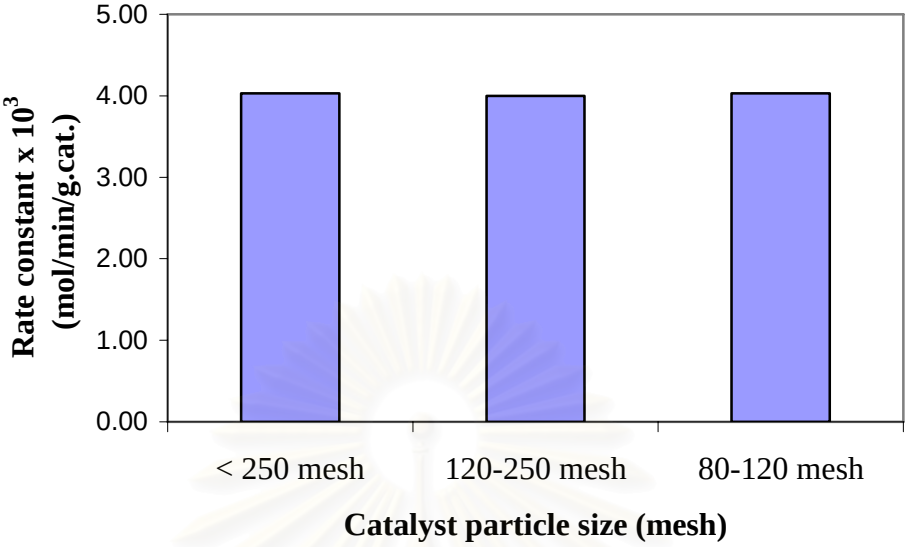

Figure 5.2 Plot of rate constant of $Pd(NO_3)_2$/MCM-41 catalysts for liquid phase hydrogenation of 1-hexene vs. catalyst particle size (Reaction conditions were 30°C, 1 atm. and 1-hexene/ethanol = 1:7)

5.1.2 Effect of Palladium Precursor

The rates of hydrogen consumption versus time-on-stream for different palladium catalysts supported on SiO_2 and MCM-41 are shown in Figure 5.3 and 5.4, respectively. Since the reaction is usually found to be zeroth order of both hydrogen and 1-hexene (Istvan Palinko 1995, Panpranot *et al.,* 2004) the slope of the line at the beginning represent both initial rate and rate constant of the reaction. The rate constant of the different supported Pd catalysts in liquid phase hydrogenation of 1-hexene at 30^{o}C and the turnover frequencies are reported in Table 5.1. For a given type of silica support, the activities of the catalyst were found to be in the order $PdCl_2$ >> $Pd(NO_3)_2$ ≈ $Pd(OAc)_2$. The turnover frequencies were calculated using the number of surface metal atoms measured by CO-chemisorption (details in section 5.2). Since the TOFs were not significantly different for all the catalysts, it is confirmed that the internal resistance due to diffusion within the pores of the reactant species did not have a significant impact on the catalytic activity of the catalysts under the reaction conditions used.

Effect of Pd precursors on the catalyst activity in hydrogenation reaction has been reported by many groups (Shen *et al.*, 2000 and 2001, Ali and Goodwin, 1998, Mahata and Vishwanathan, 2000 and Gotti and Prins, 1998). Pd catalysts supported on CeO_2 (Shen et al., 2000), SiO_2 or Al_2O_3 (Ali and Goodwin, 1998) prepared from $PdCl_2$ showed higher activities than those prepared from $Pd(NO_3)_2$ for gas phase CO hydrogenation. Mahata and Vishwanathan (2000) reported that $Pd(OOCCH_3)_2$ offered better dispersion of Pd than $PdCl_2$ or $Pd(NH_3)_4Cl_2$ on alumina. Phenol hydrogenation activity over these catalysts was found to be directly a function of available palladium surface area. Recently, in catalytic reduction of NO to N_2 over supported Pd catalysts, Pd catalysts supported on EDTA-activated γ-Al_2O_3 derived from $Pd(NO_3)_2$ were found to exhibit higher activities than those prepared from $PdCl_2$ (Nazimak *et al.,* 2004). It can be seen that there were some contradictions for the influence of palladium precursor on activity of supported Pd catalysts reported in the literature. Thus, besides the Pd metal particle size and Pd dispersion, the precursor- and/or the metal-support interaction may also play

an important role on the catalytic properties of supported Pd catalysts in hydrogenation reaction.

It should be noted that when chloride-containing compounds were used as the catalyst precursor, the presence of residual chloride has been found occasionally in supported metal catalysts (Johnston *et al,*. 1993 and Zhou *et al.*, 1994) and the catalyst activity decreased. However, in this work the catalysts prepared from $PdCl_2$ was found to exhibit higher hydrogenation activities than the ones prepared from $Pd(NO_3)_2$ or $Pd(OAc)_2$ thus there was probably no residual chloride blocking the palladium sites. It is known that residual chloride can be significantly removed during reduction procedure especially when water vapor is produced. The amounts of chloride content are shown in Table 5.1.

Table 5.1 Chloride content of fresh silica supported $PdCl_2$ catalyst

Fresh catalysts	**Chloride content (g)**	
	Initial[a]	**After impregnation and calcinations[b]**
$PdCl_2/SiO_2$	0.0038	0.0003
$PdCl_2$/MCM-41	0.0031	0.0004

[a] Based on the amount of chloride in $PdCl_2$ used.

[b] From AAS results.

It can be seen that large amount of chloride have already been removed during the impregnation and calcination steps. The chloride may be removed during heating of the solution of $PdCl_2$ in HCl at 80 ^{o}C before impregnation on the support.

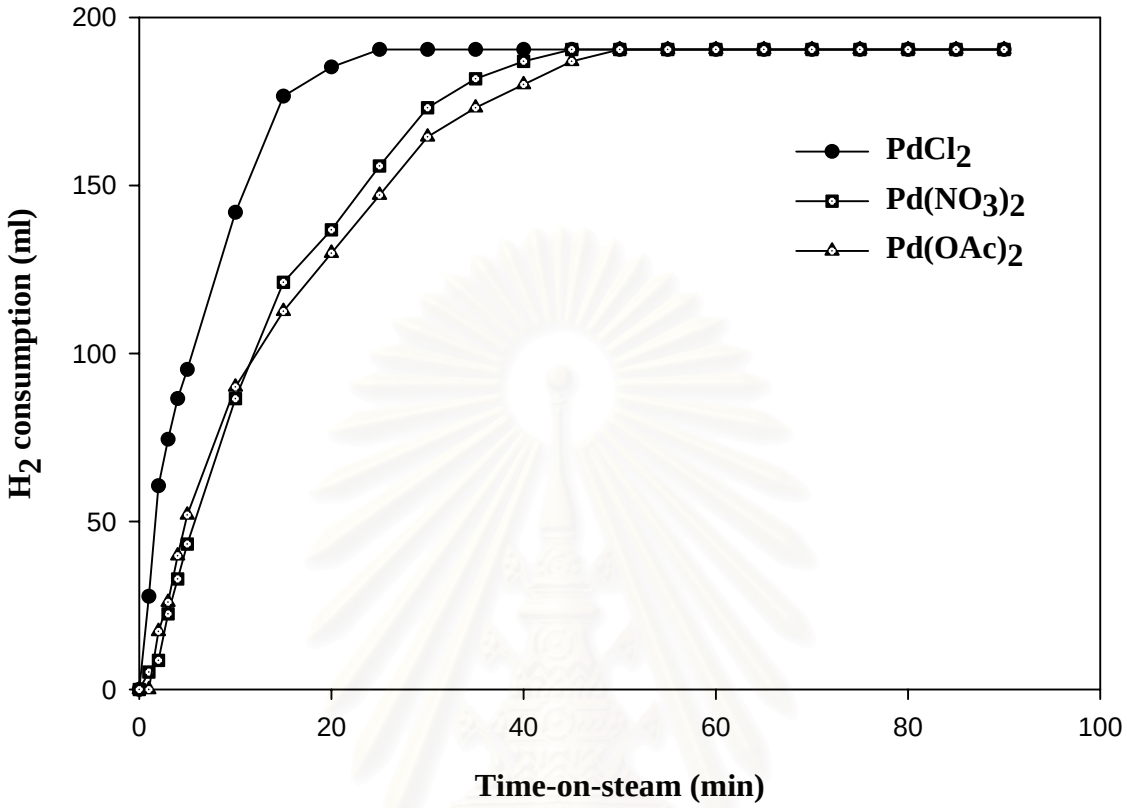

Figure 5.3 Consumption of hydrogenation as a function of time-on-stream for the hydrogenation of 1-hexene over SiO_2- supported Pd catalysts (Reaction conditions were 30^{o}C, 1 atm. and 1-hexene/ethanol = 1:7)

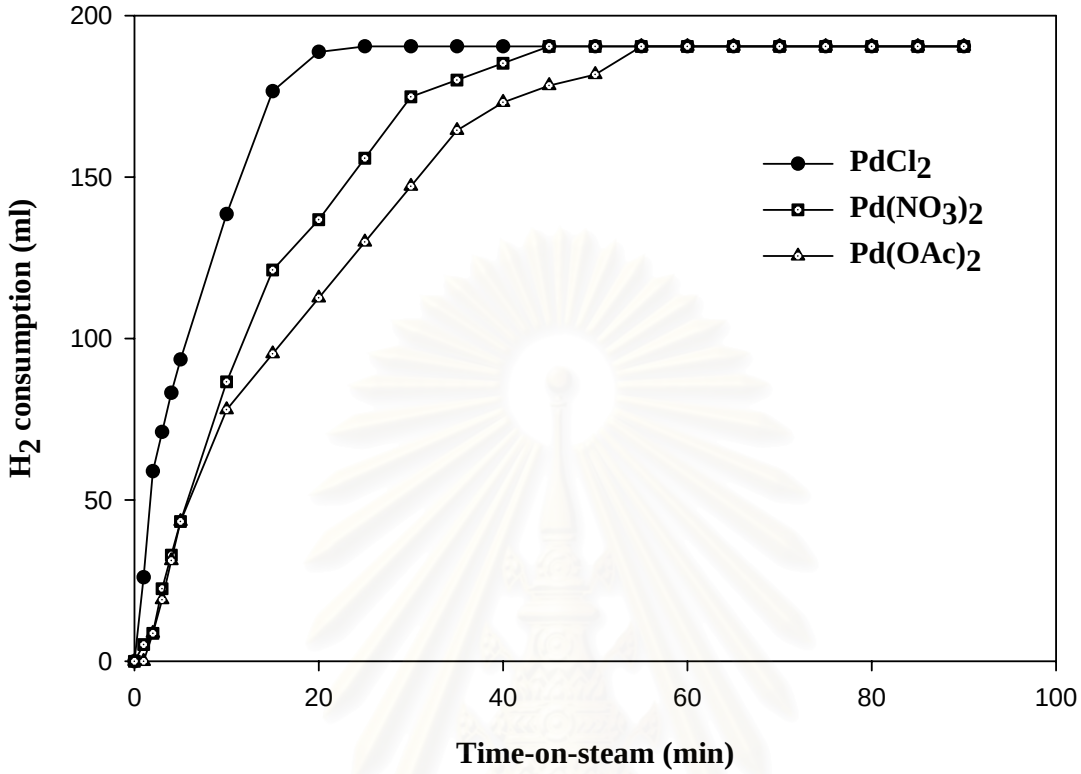

Figure 5.4 Consumption of hydrogenation as a function of time-on-stream for the hydrogenation of 1-hexene over MCM-41- supported Pd catalysts (Reaction conditions were 30^{o}C, 1 atm. and 1-hexene/ethanol = 1:7)

Table 5.2 Catalytic activities* of various SiO_2 and MCM-41 supported Pd catalyst in liquid phase hydrogenation of 1-hexene

Catalyst	**Rate constant x 10^3 (mol/min/ g cat.)**	**Turnover Frequencies (s^{-1})**
$Pd(OAc)_2/SiO_2$	5.0	12.08
$Pd(NO_3)/SiO_2$	4.0	10.01
$PdCl_2/SiO_2$	8.5	10.15
$Pd(OAc)_2$/MCM-41	4.1	9.96
$Pd(NO_3)_2$/MCM-41	4.0	11.50
$PdCl_2$/MCM-41	8.3	10.37

* Reaction conditions were 30°C, 1 atm. and 1-hexene/ethanol = 1:7

The turnover frequencies (TOF) were calculated using the active sites measured by pulse CO-chemisorption. TOF(s) were defined as:

$$TOF = \frac{\text{rate}}{\text{(numbers of active site)}}$$

$$= \frac{[\text{mole } H_2 \text{ consumed}]}{[\text{g cat.}]\,[\text{min}]} \Big| \frac{[\text{g cat.}]}{[\text{mol active site}]} \Big| \frac{[\text{min}]}{[\text{s}]}$$

$$= [s^{-1}]$$

5.2 Characterization of the Catalysts Before and After Liquid Phase Hydrogenation Reaction

5.2.1 N_2 Physisorption

The most common procedure for determining the surface area of a solid and its pore size distribution is based on adsorption and condensation of N_2 at liquid N_2 temperature using static vacuum procedure. This method is also called BET (Brunauer Emmett Teller) method.

The BET surface areas of the original supports and the catalysts are given in Table 5.2. Two types of silica (SiO_2 and MCM-41) used in this study possess high BET surface areas of ca. 716 and 921 and pore volume of ca. 0.39 and 0.87 m^3/g, respectively. Figure 1 shows the pore size distribution of the supports. A narrow pore size distribution of pore diameter ca. 3 nm was observed for both supports. Impregnation of silica with palladium followed by calcination at 500^oC resulted in significant decreases in the BET surface areas of the supports suggesting that palladium was deposited in some of the pores of the supports.

Table 5.3 N_2 Physisorption Results

Catalysts	BET S.A.[a] m^2/g
Support	
SiO_2	716
MCM-41	921
Fresh catalysts	
$Pd(OAc)_2/SiO_2$	444
$Pd(NO_3)/SiO_2$	381
$PdCl_2/SiO_2$	516
$Pd(OAc)_2$/MCM-41	342
$Pd(NO_3)_2$/MCM-41	670
$PdCl_2$/MCM-41	528

[a] Error of measurement was ± 5%.

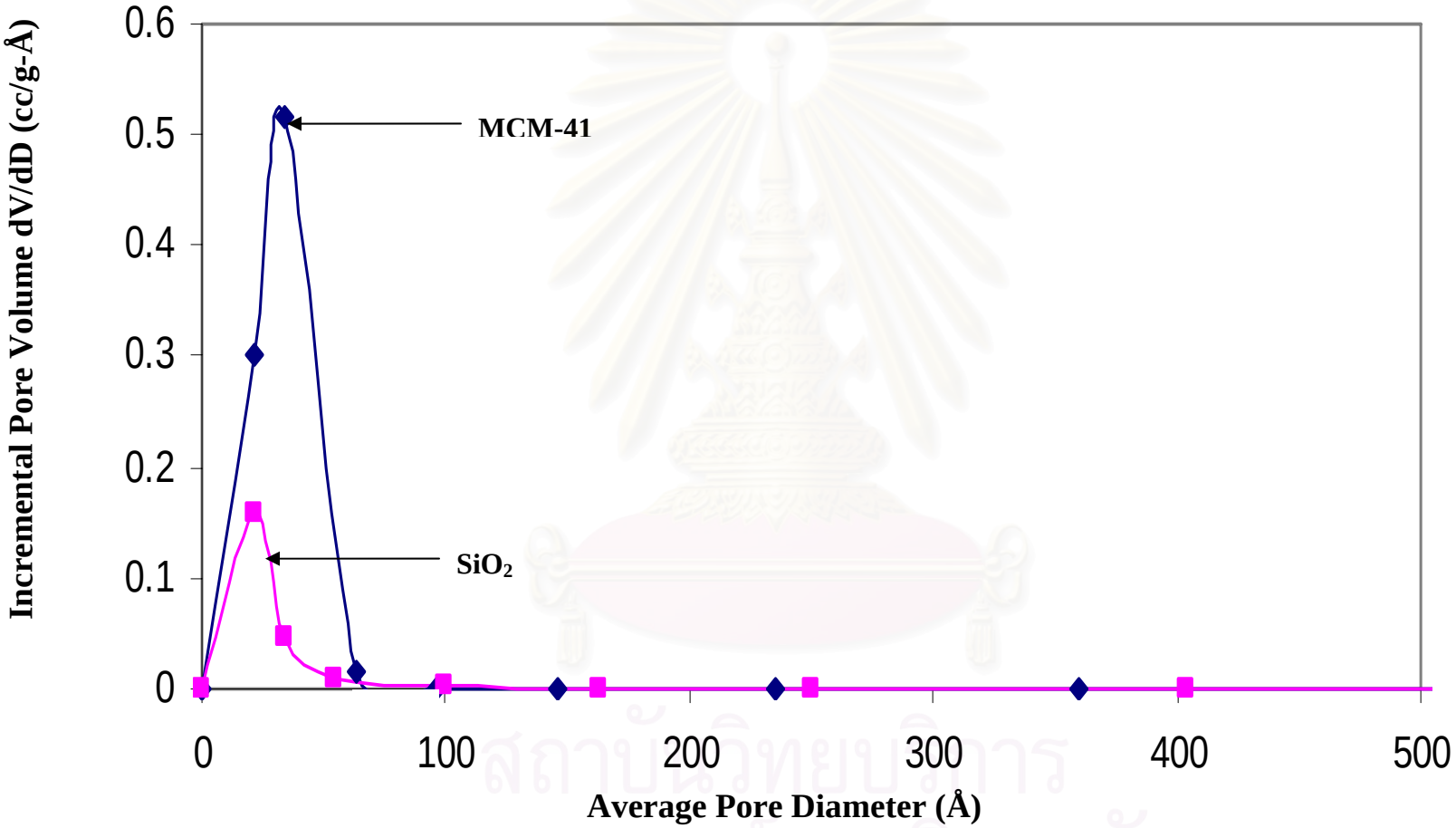

Figure 5.5 Pore size distribution of SiO_2 and MCM-41-supported Pd catalysts.

5.2.2 X-ray diffraction (XRD)

Bulk crystal structure and chemical phase composition of a crystalline material having crystal domains of greater than 3-5 nm can be detected by diffraction of an X-ray beam as a function of the angle of the incident beam. Broadening of the diffraction peaks can be used to estimate crystallite diameter.

The X-ray diffraction patterns of the MCM-41 gave an XRD peak at low 2θ around 2.58 degrees (Figure 5.6). After impregnation of palladium the intensity of the XRD peak for the MCM-41 decreased for all the catalyst samples and the peaks became broader due probably to the structure of MCM-41 becoming less ordered by impregnation of palladium or due to secondary scattering of the X-rays. Since the major peak for MCM-41 was still observes, the structure of MCM-41 was not destroyed but the long-range order of MCM-41 may have shrunk (Pasqua *et al*., 2001).

After reaction, it was found that the intensity of the MCM-41 reflection peak further decreased after 1.5 h hydrogenation of 1-hexene at room temperature. It is suggested that the long range order of the MCM-41 may have partially collapsed during reduction and reaction and/or the greater X-ray scattering ability of sintered metal particles (Marler *et al.*, 1996).

The XRD patterns at higher diffraction angles of the silica supported palladium catalysts prepared with different palladium precursors in the calcined state are shown in Figures 5.7 and 5.8. The characteristic peaks for PdO were observed at 2θ of ca. 33.8 and less so at 42.0, 54.8, 60.7, and 71.4^{o}2θ. $PdCl_2/SiO_2$ and $PdCl_2$/MCM-41 exhibited very small XRD peaks. This suggests that the crystallite size of palladium oxide prepared from palladium chloride on SiO_2 and MCM-41 may be below the lower limit for XRD detectability (3-5 nm).

The PdO particle sizes were calculated from XRD line broadening of the peak at 33.8 ^{o} 2θ using Scherrer's equation (Klug and Alexander, 1974) and are reported in Table 5.4. The PdO particle sizes for a given silica support were found to be in the order of $PdCl_2$ < $Pd(NO_3)_2$ < $Pd(OAc)_2$. The differences in PdO particle sizes on different supports can be ascribed to differences induced by both the support and Pd precursor on sintering of palladium during preparation (Panpranot *et al.*, 2004). For both Pd/SiO_2 and Pd/MCM-41 prepared from $Pd(NO_3)_2$ and $Pd(OAc)_2$, the PdO particles were found to be ca. 10-13 nm. These palladium particles were much larger than the average pore diameter of MCM-41 (3 nm), suggesting that using palladium acetate and palladium nitrate precursors to prepare SiO_2 and MCM-41-supported Pd catalysts by incipient wetness impregnation resulted in some large palladium oxide particles deposited on the external surface of the supports.

After reaction, the recovered catalysts were re-calcined in air at 500 ºC for 2 hours in order to remove any carbon deposit after reaction. The XRD patterns at higher diffraction angles of the silica supported Pd catalysts in the re-calcined state are shown in Figure 5.9 and Figure 5.10. It was found that the PdO particle sizes for all the catalyst samples became larger, indicating that palladium metal particles sintered after reaction and re-calcination. XRD pattern of the spent Pd/SiO_2 and Pd/MCM-41 catalysts showed significant peaks at 2θ of ca. 33.8 ^{o} 2θ. It was found that the smaller PdO particles obtained from $PdCl_2$ resulted in greater Pd sintering while the particle sizes of $Pd(NO_3)_2$ and $Pd(OAc)_2$ were not significantly changed. Sintering of metal particles after reduction and reaction during liquid phase hydrogenation has been reported earlier by Choudary *et al.*, 1999 and Dominguez-Quintero *et al.*, 2003. Sintering of supported metal particles is typically irreversible and can occur even at ambient temperature because of atomic migration process involving the extraction and transport of surface metal atoms by chelating molecules (Besson et al., 2003)

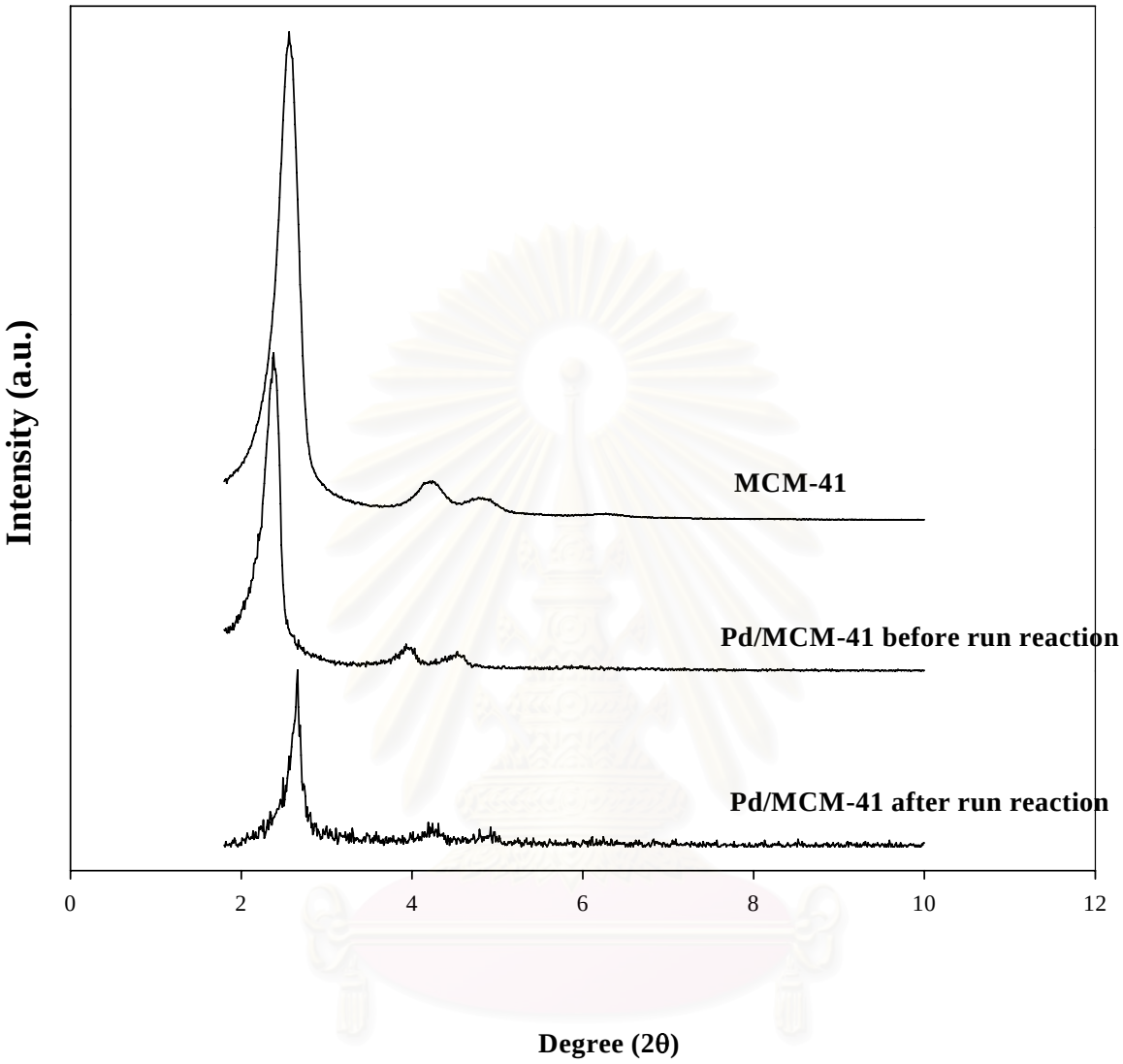

Figure 5.6 XRD patterns of MCM-41 and MCM-41 supported Pd catalysts before and after run reaction at low 2θ degrees

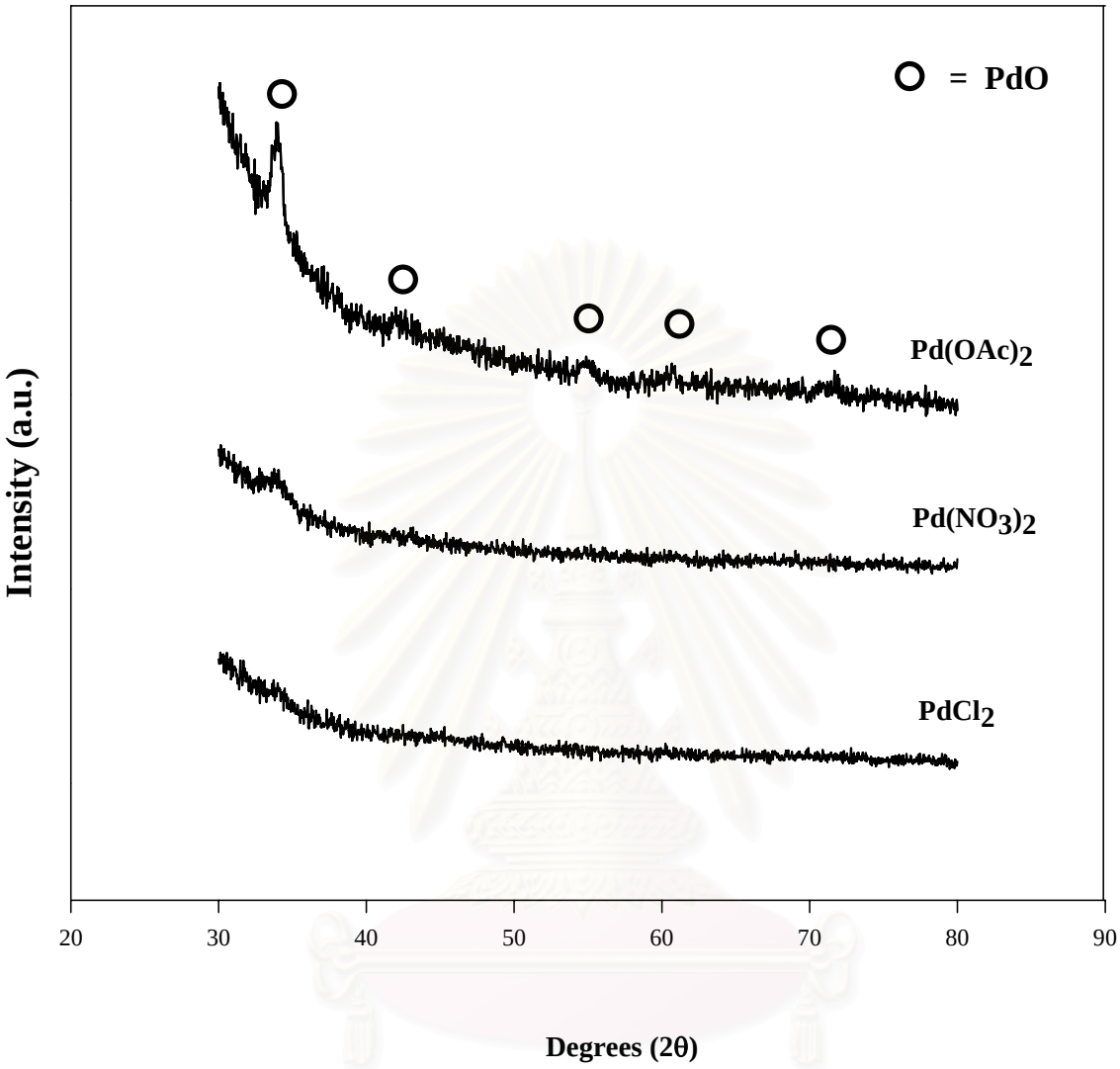

Figure 5.7 Effect of palladium precursors on the XRD patterns of fresh Pd/SiO_2 catalysts at high 2θ degrees

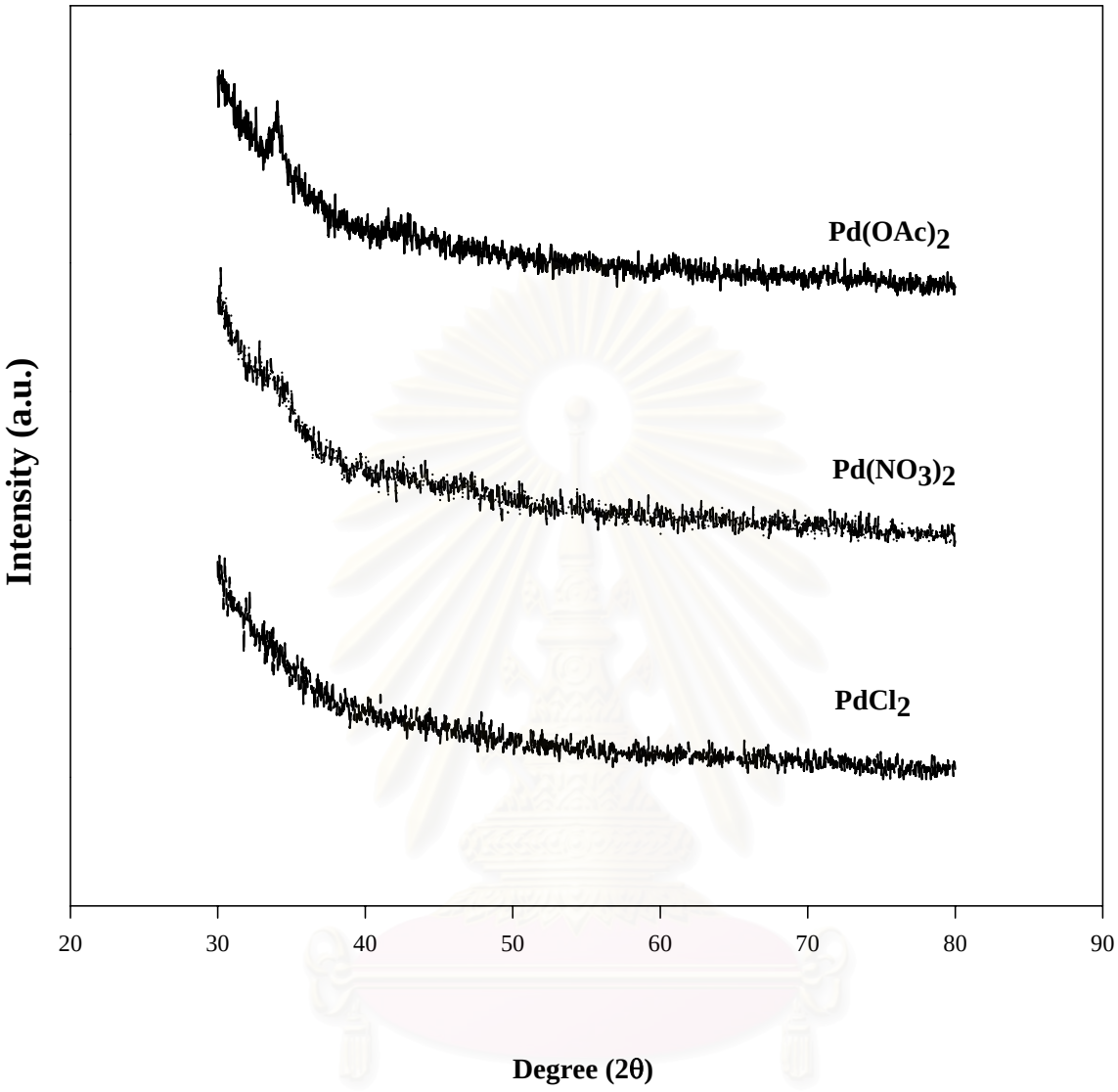

Figure 5.8 Effect of palladium precursors on the XRD patterns of fresh Pd/MCM-41 catalysts at high 2θ degrees

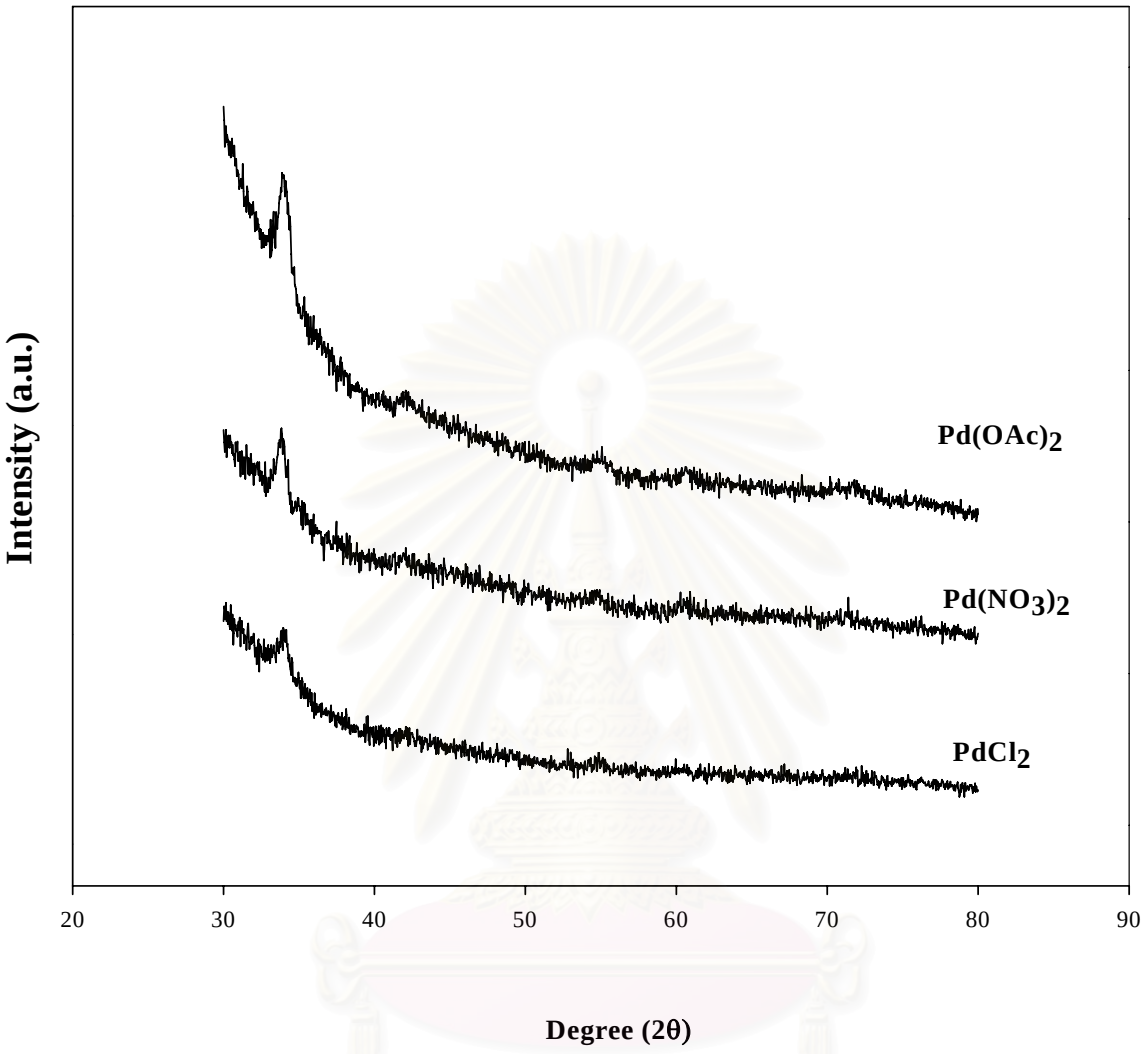

Figure 5.9 XRD patterns of spent Pd/SiO_2 catalysts at high 2θ degrees

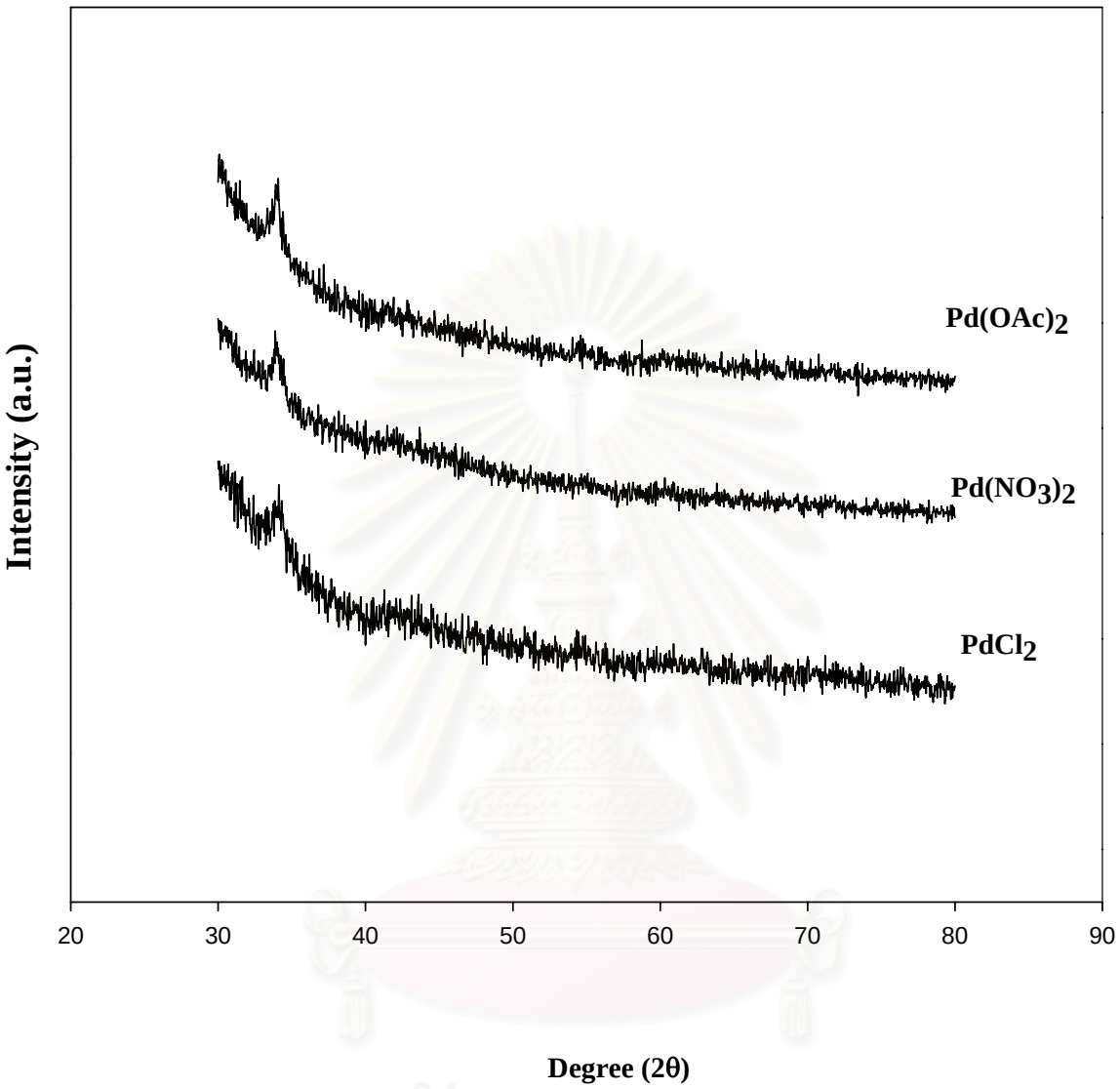

Figure 5.10 XRD patterns of spent MCM-41 catalysts at high 2θ degrees

Table 5.4 Average PdO particle size based on XRD results

Catalyst	Average PdO Particle Diameter (nm)	
	Fresh	**Spent***
$Pd(OAc)_2/SiO_2$	12.00	12.70
$Pd(NO_3)_2/SiO_2$	10.00	12.64
$PdCl_2/SiO_2$	<3	11.36
$Pd(OAc)_2$/MCM-41	13.00	14.46
$Pd(NO_3)_2$/MCM-41	9.45	13.64
$PdCl_2$/MCM-41	<3	10.54

* After hydrogenation of 1-hexene (30^oC, 1 atm. and 1-hexene/ethnol = 1:7)

5.2.3 Transmission Electron Microscopy (TEM)

TEM micrographs were taken for all the catalysts in order to physically measure the size of palladium oxide particles and/or palladium clusters and size distribution of supported metals. It allows determination of the micro-texture and microstructure of electron transparent samples by transmission of a focused parallel electron beam to a fluorescent screen with a resolution presently better than 0.2 nm. Although TEM measurements were only done for a very small portion of each catalyst, the results are able to provide further evidence about Pd dispersion. The TEM micrographs for fresh and spent catalyst (after reaction and re-calcined) of SiO_2- and MCM-41- supported Pd catalysts are shown in Figure 5.11 - 5.13 and 5.14 – 5.16, respectively. In order to avoid the influence of carbon deposits on the pore structure and the contrast of TEM images, after being taken out from the reactor and dried at room temperature, the catalysts were re-calcined in air at 500^{o}C for 2 h before characterization to remove any carbon deposits. TEM images were found to be in accordance with the results obtained from XRD. The particle size of PdO particles measured from TEM images (Table 5.4) before and after reaction was found to be in the order of $Pd(OAc)_2 \approx Pd(NO_3)_2 >> PdCl_2$. The Pd dispersion of palladium on fresh catalyst for a given support was in the order of $PdCl_2 >> Pd(NO_3)_2 \approx Pd(OAc)_2$. For the spent catalysts, both SiO_2 and MCM-41 resulted in larger palladium oxide particles with $PdCl_2/SiO_2$ and $PdCl_2$/MCM-41 exhibited the most sintering.

Sintering probability can be higher when a metal particle was located closed to other ones. It is known that temperature, atmosphere, metal type and metal dispersion, promoters/impurities, and support surface area, texture and porosity are the principle parameters affecting rates of sintering (Farrauto and Bartholomew, 1997). However, the mechanism of metal sintering in liquid phase reaction has not well been investigated so far. Arai *et al.* has proposed that sintering occurs through transport of Pd metal between support and solvent as well as transport on the support during Heck coupling reaction (Zhou *et al.*, 2000).

Table 5.5 TEM results

Catalyst	PdO Particle Diameter (nm)	
	Fresh	**Spent***
$Pd(OAc)_2/SiO_2$	11.50	12.37
$Pd(NO_3)_2/SiO_2$	10.10	12.00
$PdCl_2/SiO_2$	4.76	9.56
$Pd(OAc)_2$/MCM-41	12.00	13.10
$Pd(NO_3)_2$/MCM-41	10.20	12.65
$PdCl_2$/MCM-41	5.12	11.36

* After hydrogenation of 1-hexene (30^oC, 1 atm. and 1-hexene/ethnol = 1:7)

(a)

(b)

Figure 5.11 TEM of $Pd(OAc)_2/SiO_2$ (a) fresh and (b) spent catalyst

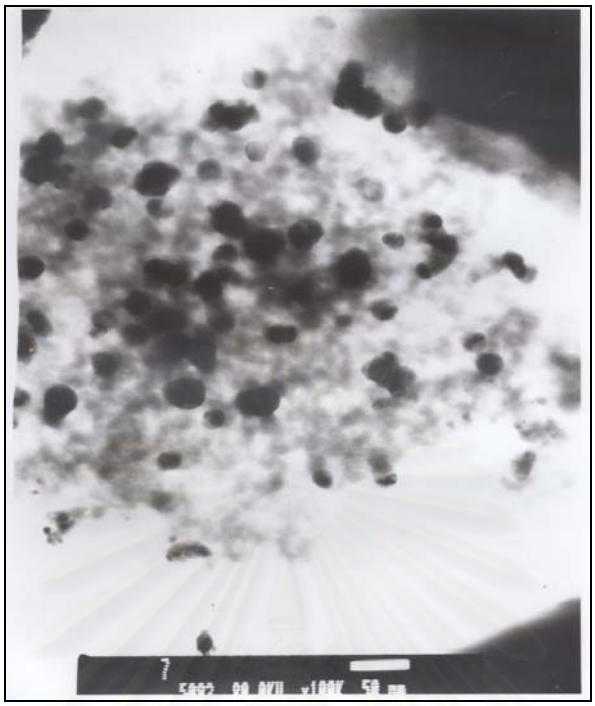

(a)

(b)

Figure 5.12 TEM of $Pd(NO_3)_2/SiO_2$ (a) fresh and (b) spent catalyst

(a)

(b)

Figure 5.13 TEM of $PdCl_2/SiO_2$ (a) fresh and (b) spent catalyst

(a)

(b)

Figure 5.14 TEM of $Pd(OAc)_2$/MCM-41 (a) fresh and (b) spent catalyst

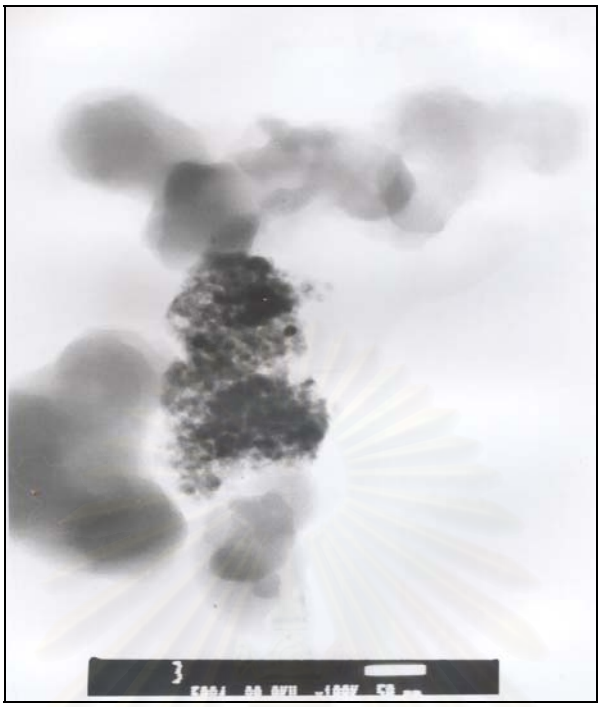

(a)

(b)

Figure 5.15 TEM of $Pd(NO_3)_2$/MCM-41 (a) fresh and (b) spent catalyst

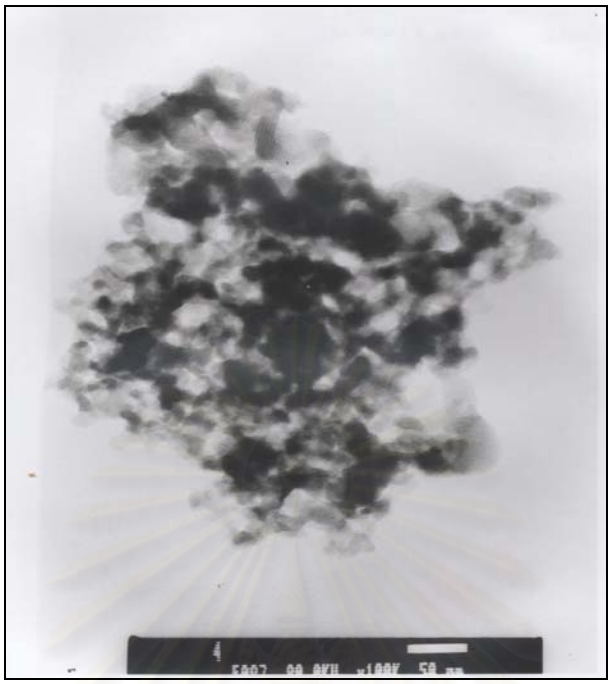

(a)

(b)

Figure 5.16 TEM of $PdCl_2$/MCM-41 (a) fresh and (b) spent catalyst

5.2.4 Scanning Electron Microscopy (SEM)

Scanning electron microscopy (SEM) is a powerful tool for observing directly surface texture and morphology of catalyst materials. In the backscattering scanning mode, the electron beam focused on the sample is scanned by a set of deflection coils. Backscattered electrons or secondary electrons emitted from the sample are detected.

SEM was carried out for all the catalyst samples. Figure 5.17–5.22 show SEM micrograph of the catalyst granules in the backscattering mode. The white or light spots on the catalyst granules represent a high concentration of palladium and its compounds while the darker areas of the granules indicate the silica support. The SEM micrographs show different catalyst granule sizes. For MCM-41 supported catalysts, the granule sizes were approximately 20-30 μm, whereas granule sizes of SiO_2 were around 130-150 μm. It would appear that the size and shape of the catalyst granules were not affected during liquid-phase hydrogenation reaction suggesting that the different silica supports used in this study have reasonably high attrition resistances.

A significant amount of Pd lost after reaction was also evidenced by SEM especially for the supported Pd catalysts prepared from palladium nitrate and palladium acetate. However, such phenomena was not clearly seen catalysts prepared from palladium chloride. The loss of Pd from the catalysts suggested that leaching of Pd occurred during liquid phase hydrogenation of 1-hexene. The details about metal leaching were discussed in the section of atomic absorption spectroscopy (section 5.2.5).

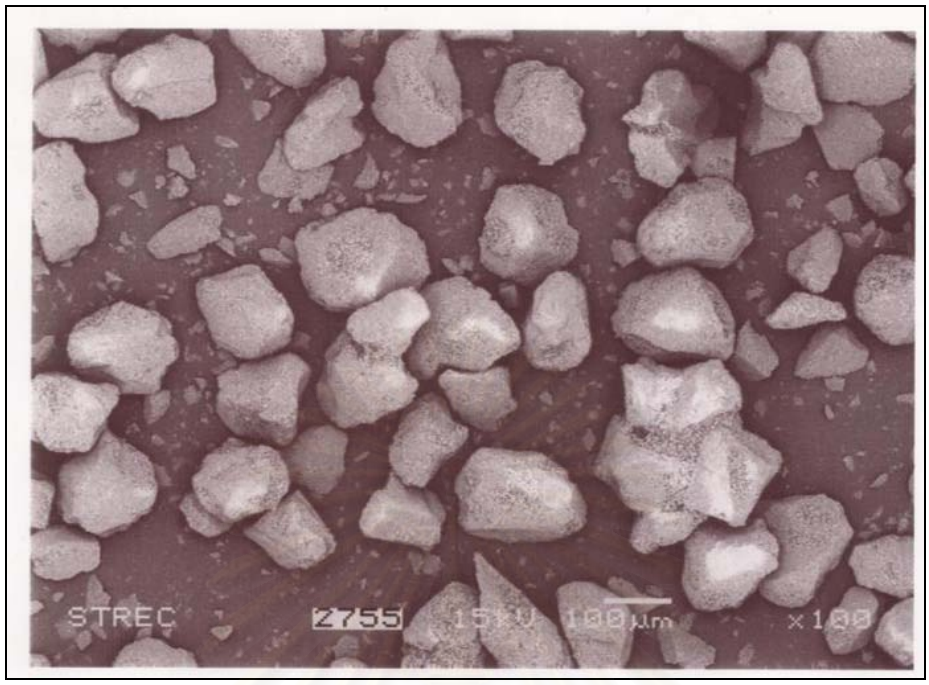

(a)

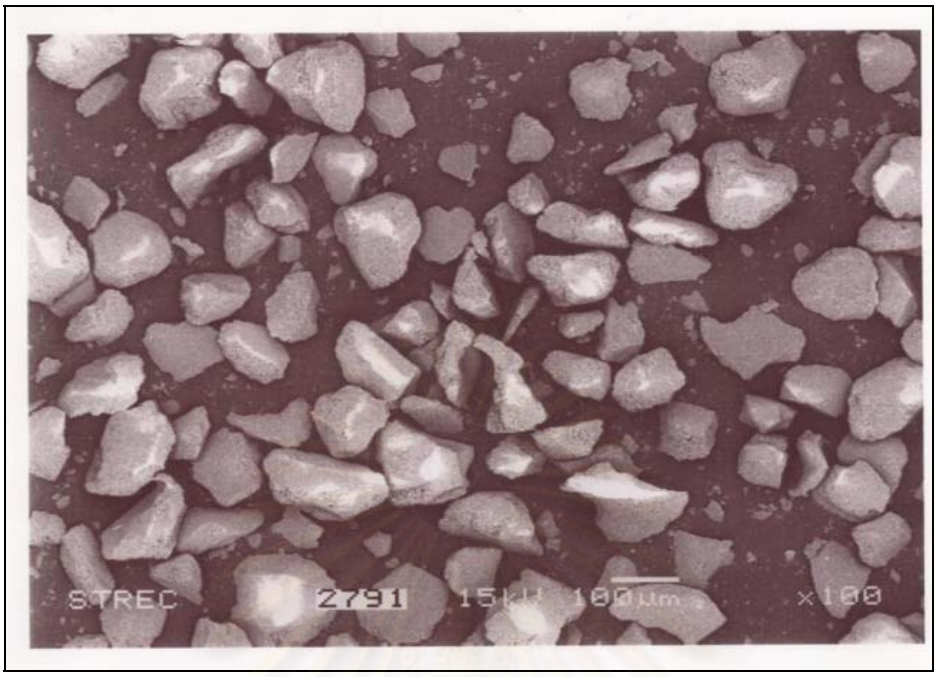

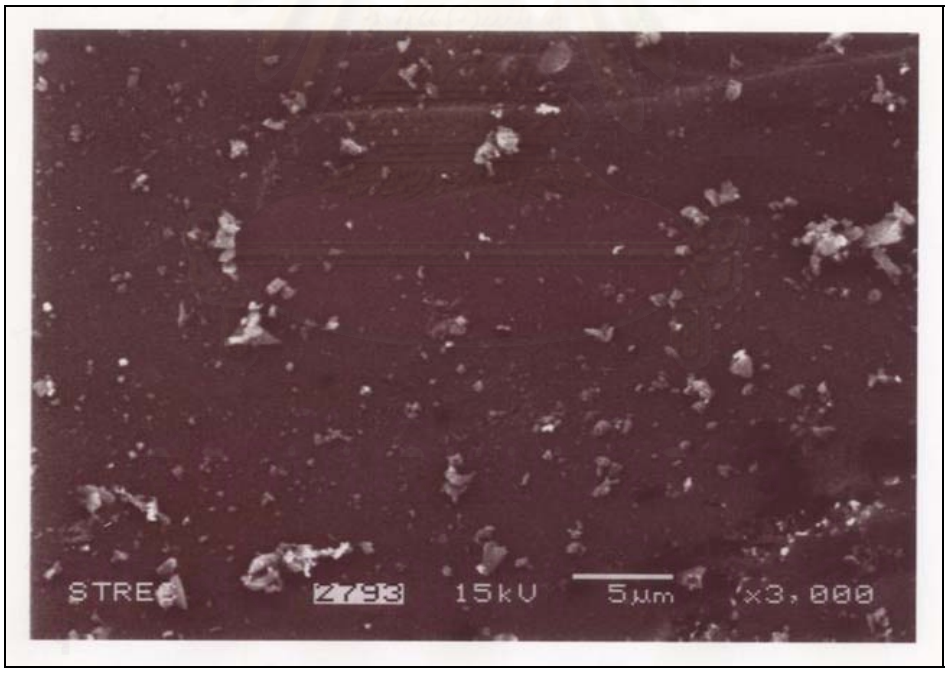

(b)

Figure 5.17 SEM Micrographs (back scanning mode) of (a) fresh and (b) spent $Pd(OAc)_2/SiO_2$

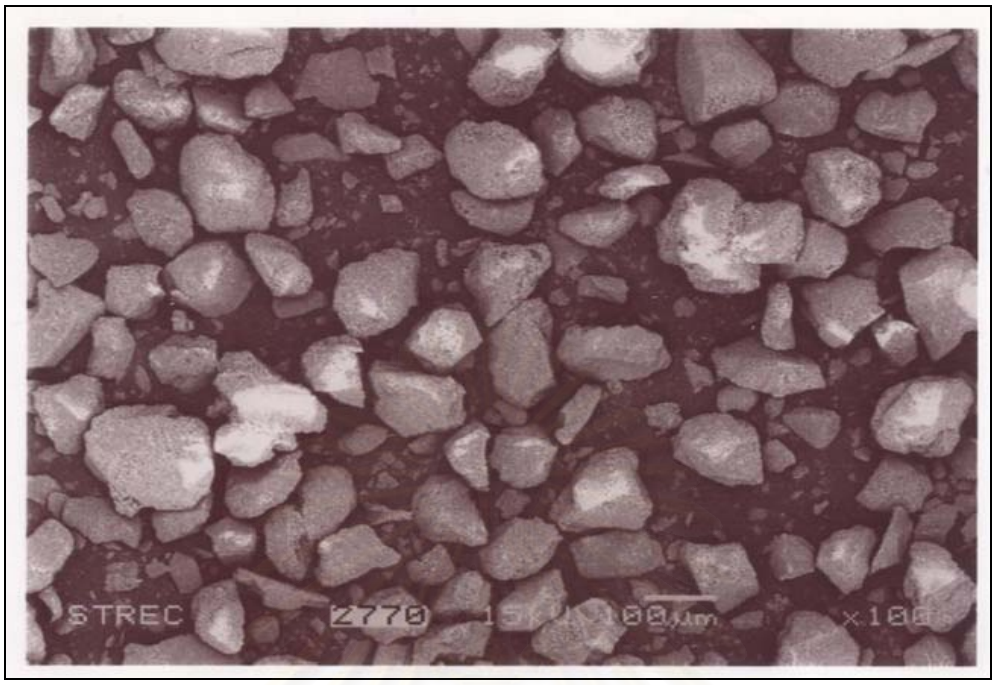

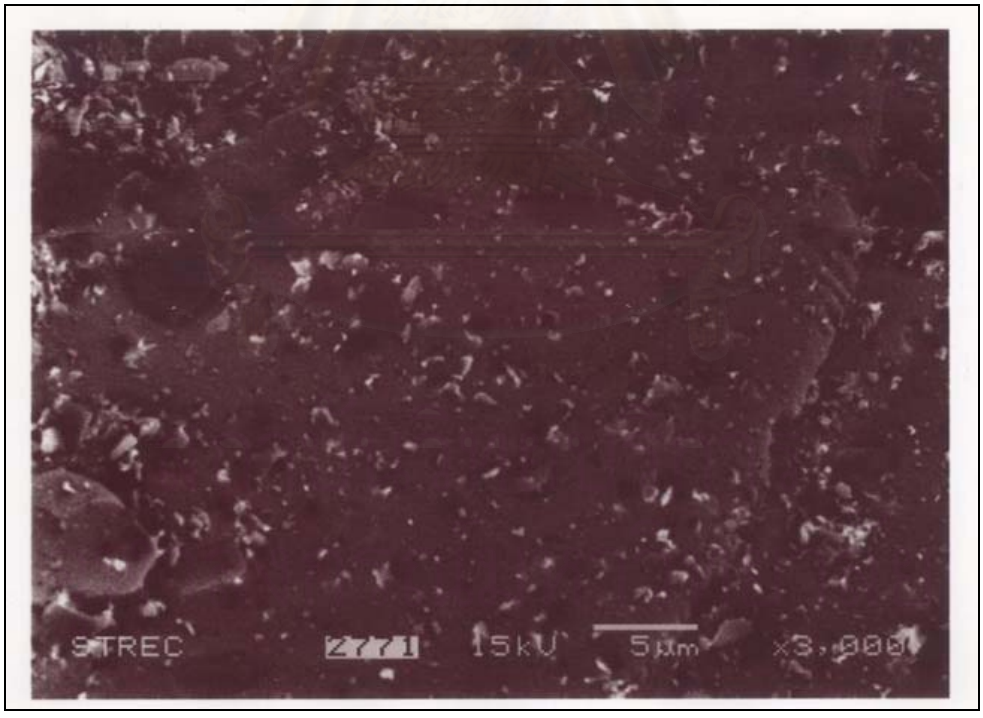

(a)

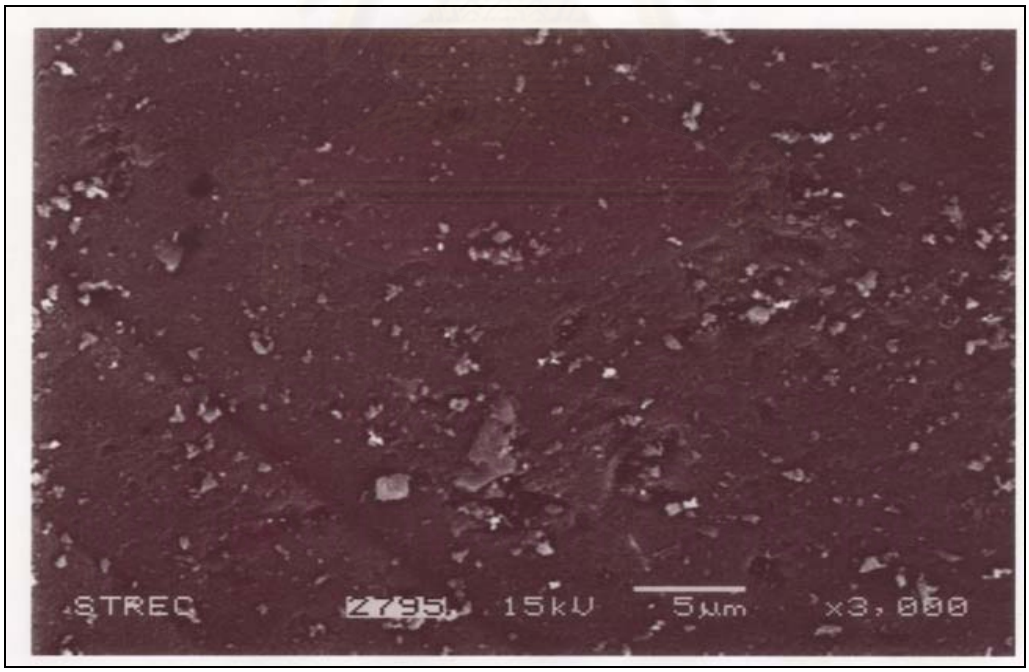

(b)

Figure 5.18 SEM Micrographs (back scanning mode) of (a) fresh and (b) spent $Pd(NO_3)_2/SiO_2$

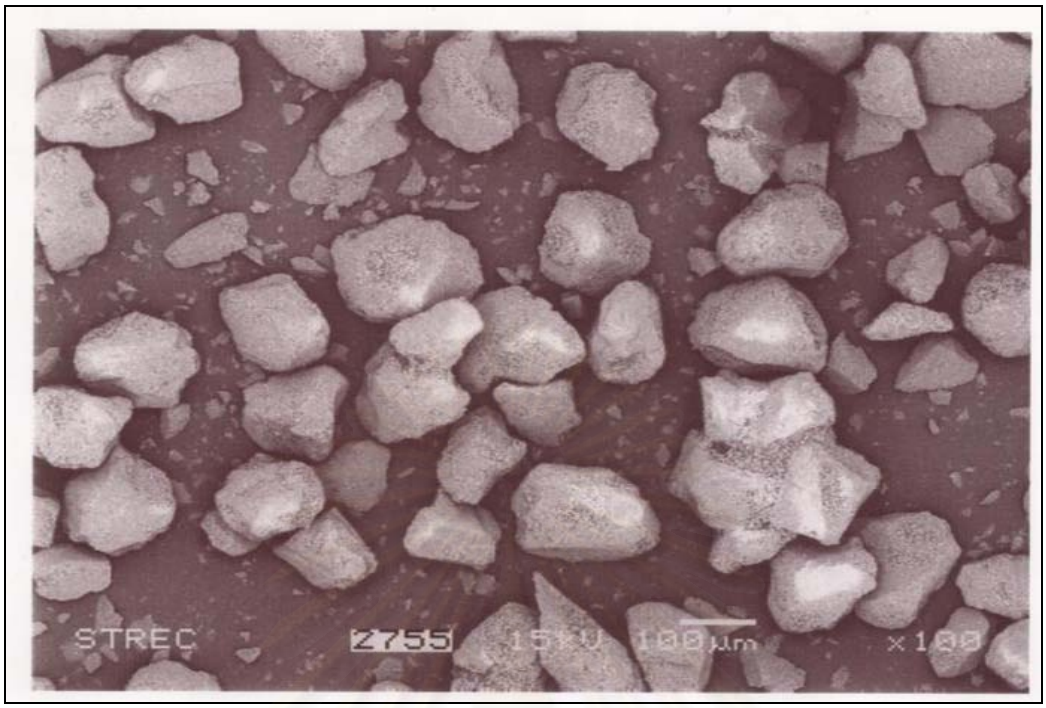

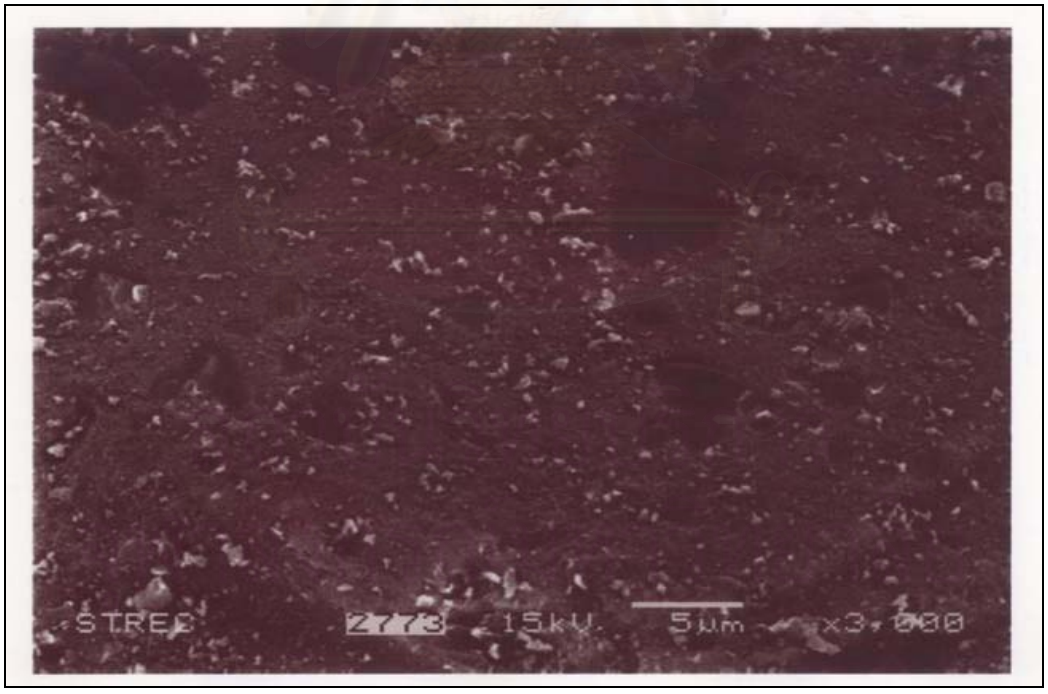

(a)

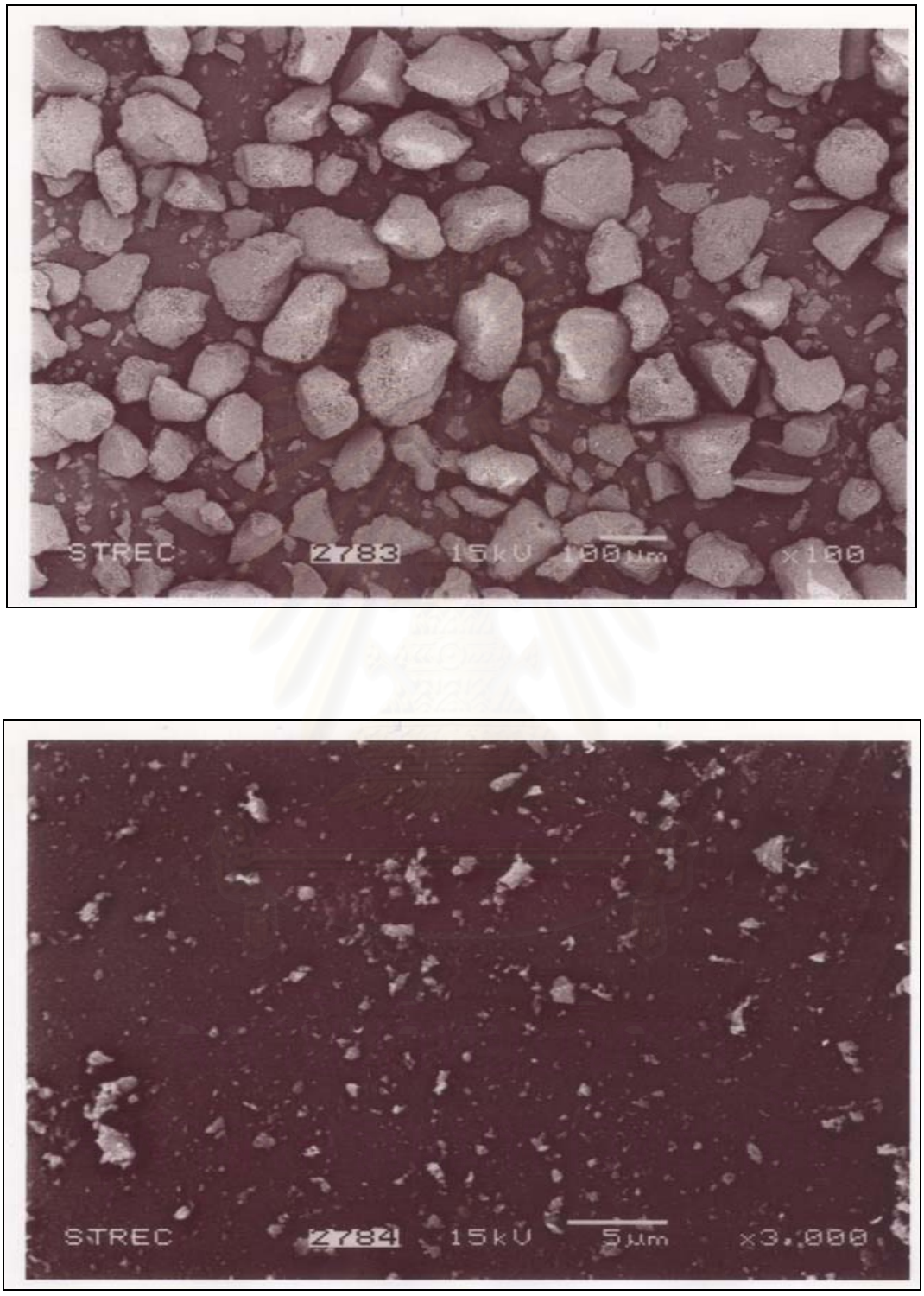

(b)

Figure 5.19 SEM Micrographs (back scanning mode) of (a) fresh and (b) spent $PdCl_2/SiO_2$

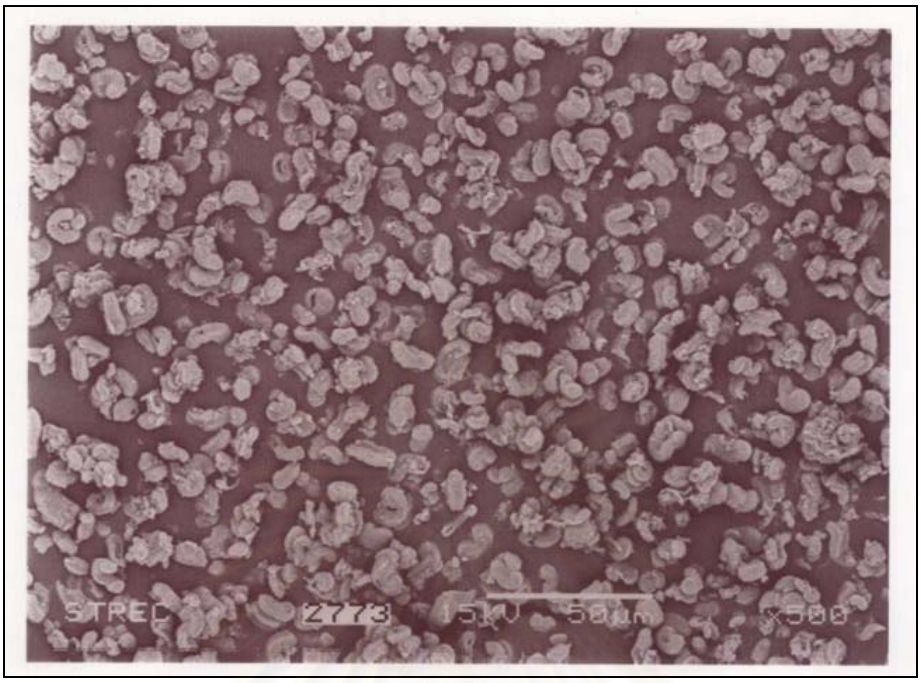

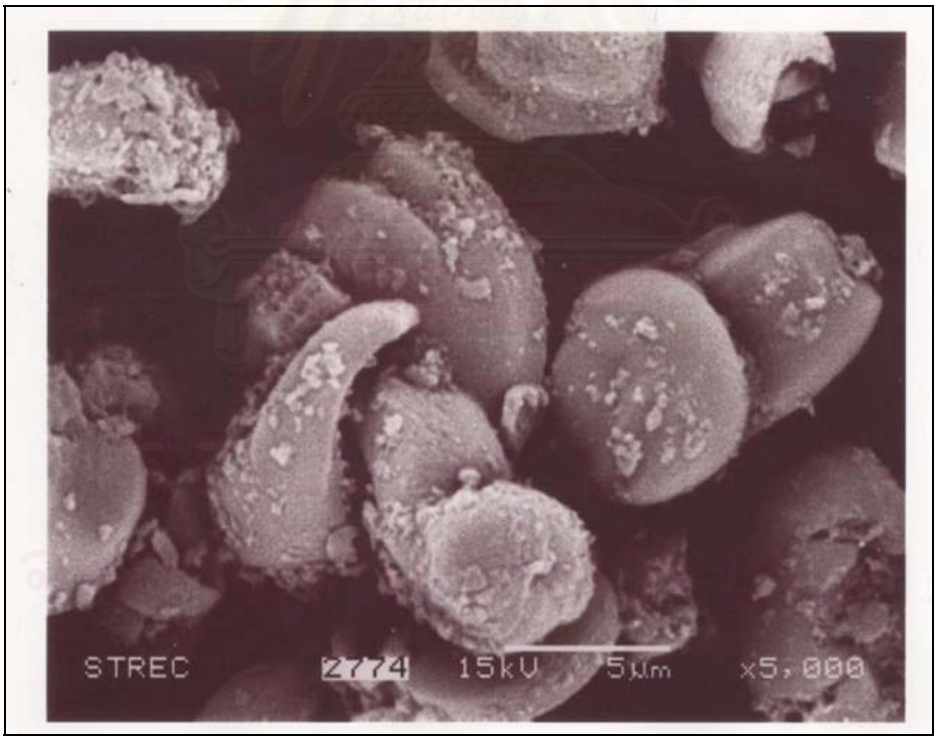

(a)

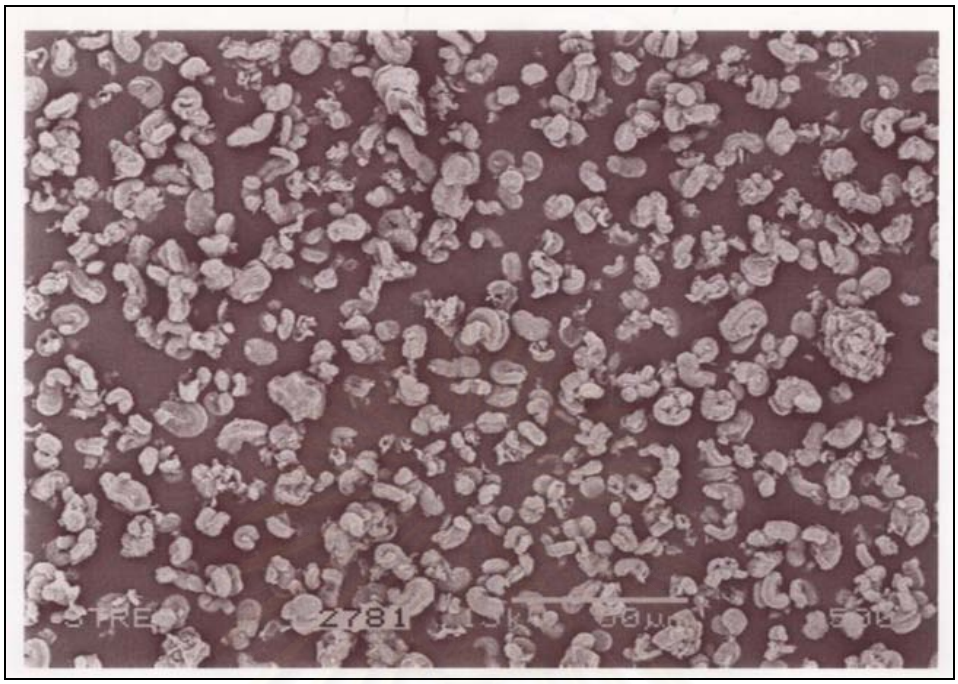

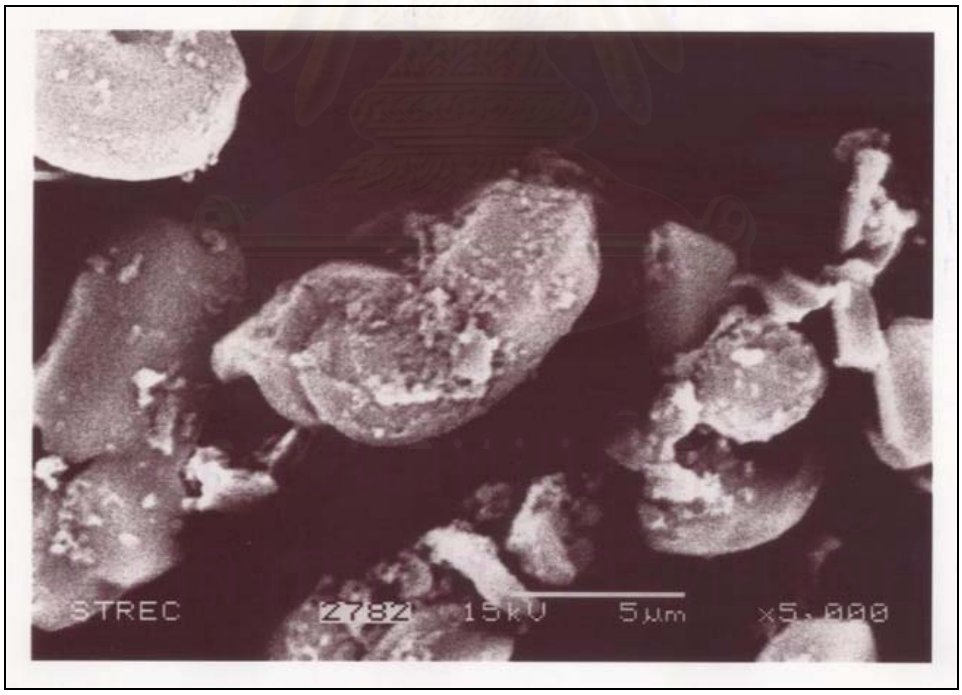

(b)

Figure 5.20 SEM Micrographs (back scanning mode) of (a) fresh and (b) spent $Pd(OAc)_2$/MCM-41

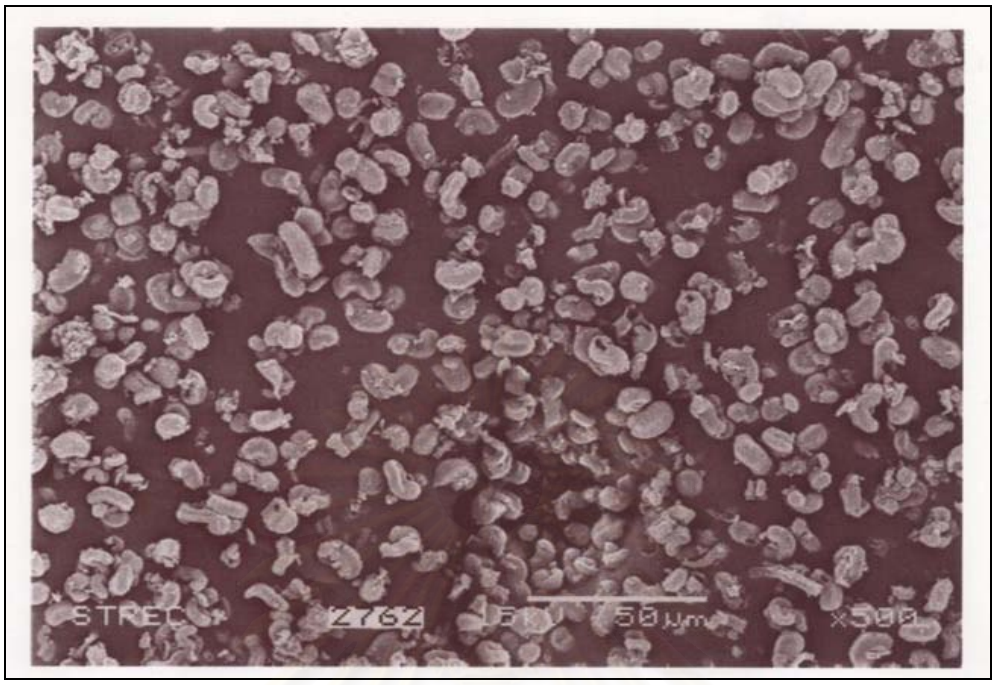

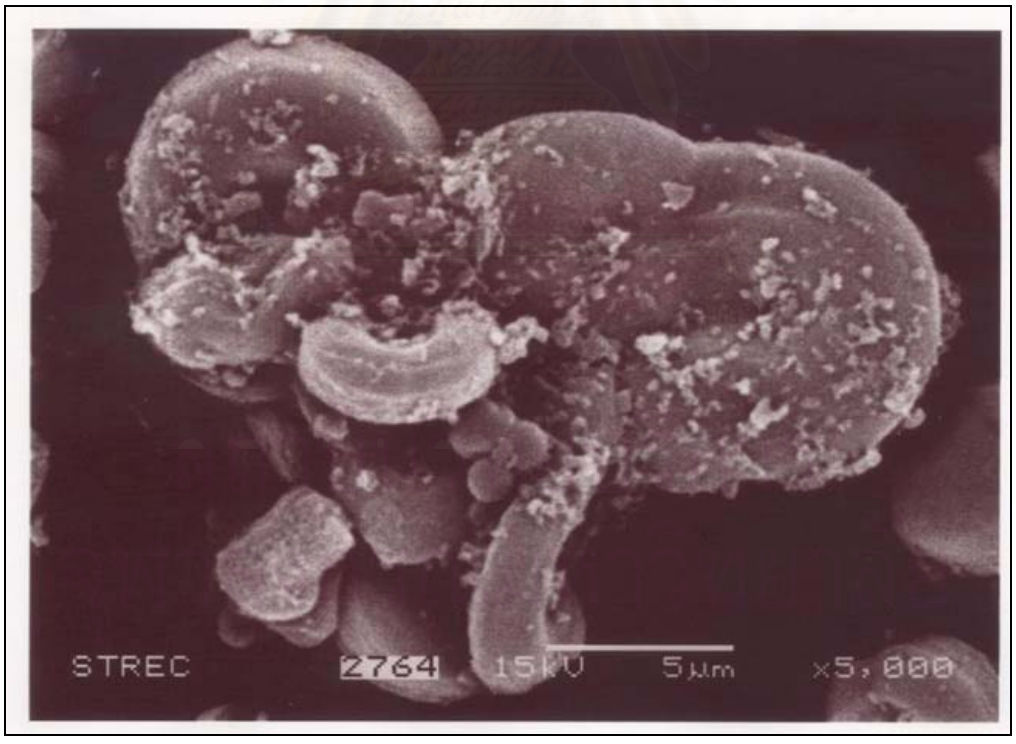

(a)

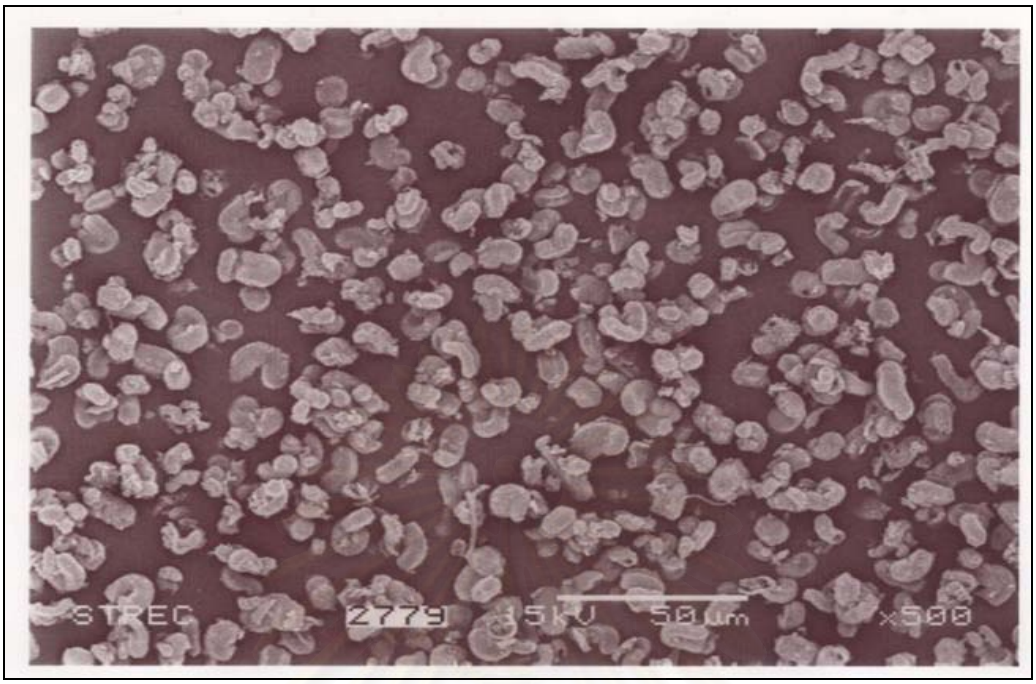

(b)

Figure 5.21 SEM Micrographs (back scanning mode) of (a) fresh and (b) spent $Pd(NO_3)_2$/MCM-41

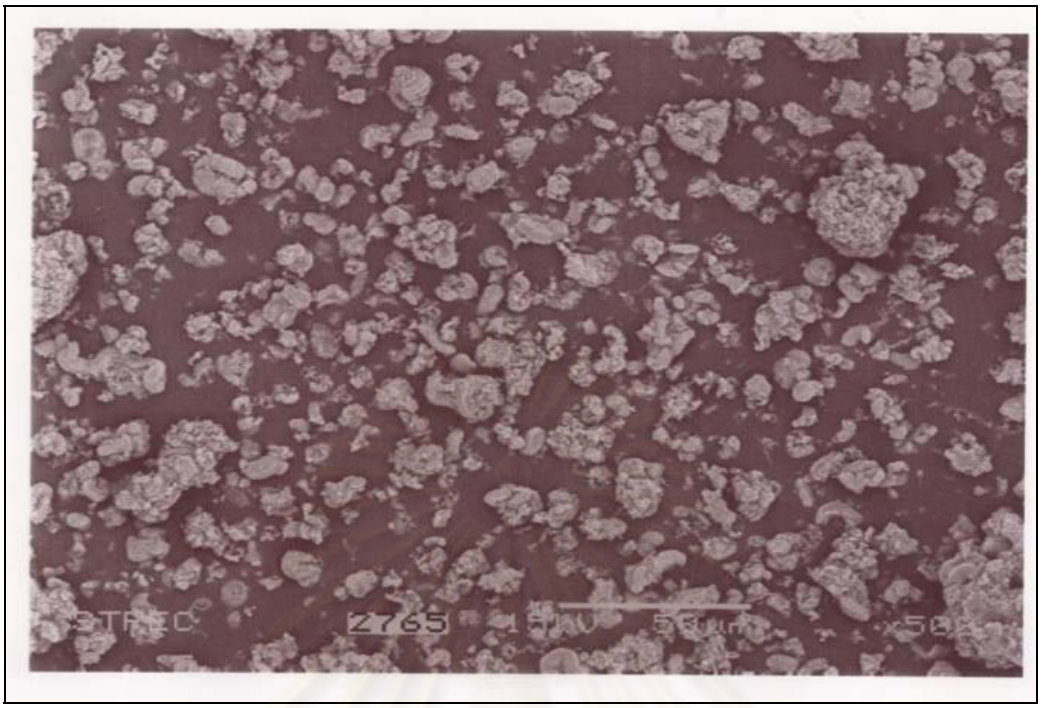

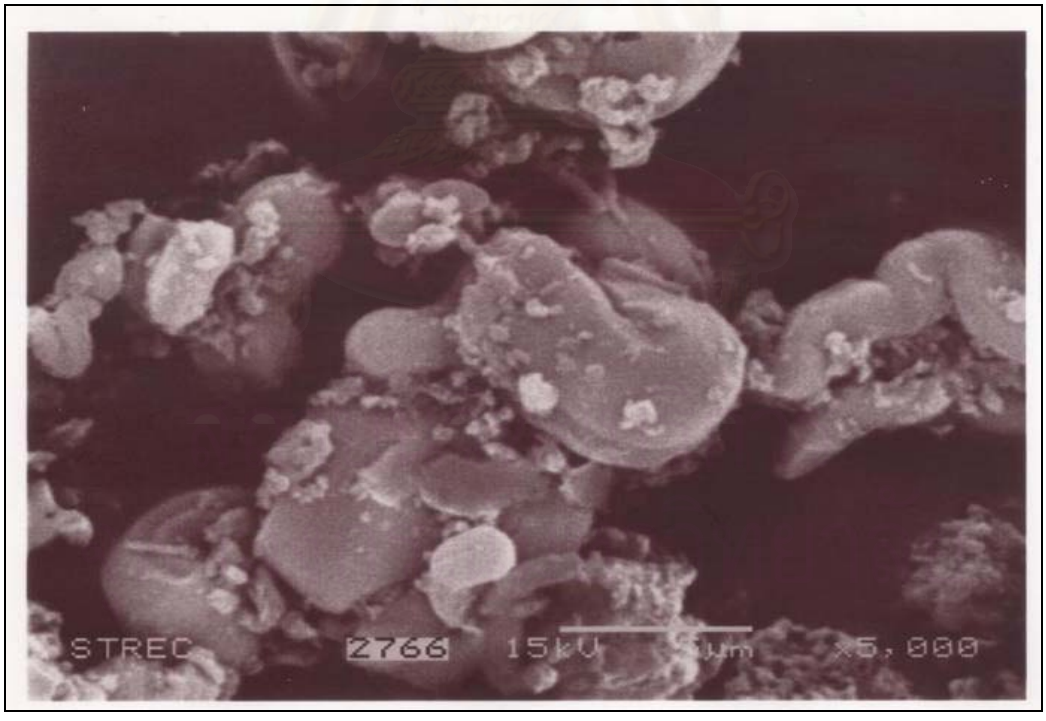

(a)

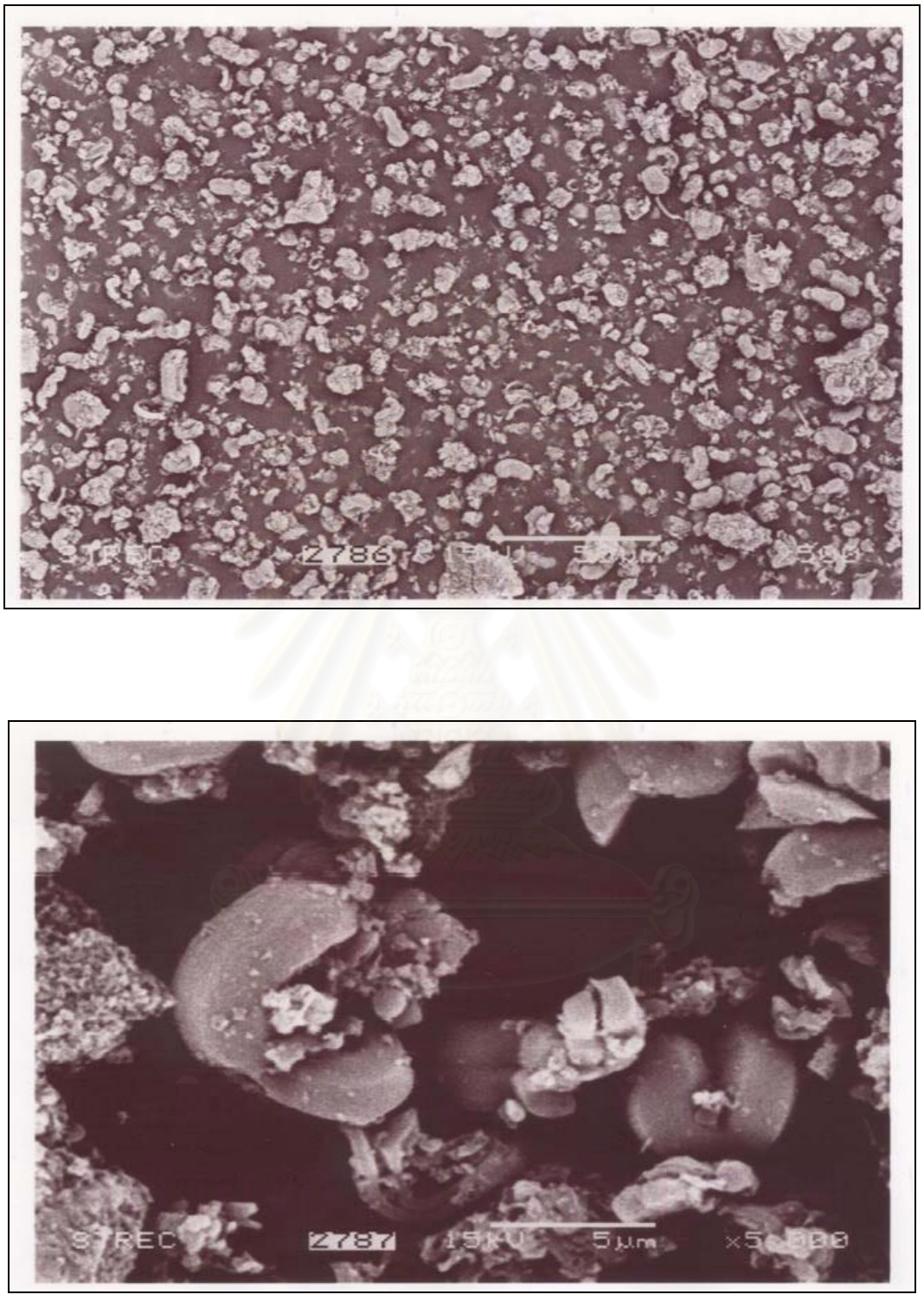

(b)

Figure 5.22 SEM Micrographs (back scanning mode) of (a) fresh and (b) spent $PdCl_2$/MCM-41

5.2.5 Atomic Absorption Spectroscopy

Atomic absorption spectroscopy is a very common technique for quantitative measurement of atomic composition based on photon absorption of a vaporized aqueous solution prepared from the starting material.

The actual amounts of palladium loading before and after reaction determined by atomic adsorption spectroscopy are given in Table 5.5. Before reaction, palladium loading on the catalyst samples was approximately 0.33-0.57 wt%. After one batch hydrogenation reactions of 1-hexene, palladium loadings decreased by 1.75-41.18 %. This indicates that leaching of palladium occurred during reaction. The order of the percentages of the amount of palladium leaching was found to be $Pd(NO_3)_2$/MCM-41 ≈ $Pd(NO_3)_2/SiO_2$ > $Pd(OAc)_2/SiO_2$ ≈ $Pd(OAc)_2$/MCM-41 >> $PdCl_2$/MCM-41 ≈ $PdCl_2/SiO_2$. Within experimental error, Pd catalysts prepared from palladium chloride showed almost no leaching of palladium into the reaction media.

Leaching of active metal is one of the main causes of catalyst deactivation in liquid phase hydrogenation reaction. The mechanism of metal leaching involves usually metal compounds that are formed that are soluble in the reaction mixture. Since it is unlikely that 1-hexene forms compound with Pd at room temperature, unless it is some hydro-organic complex. It is likely that Pd hydride formation is the cause of metal loss. It is well known that Pd particles are able to absorb H_2 within their crystal structure to form a Pd-β-hydride phase. A number of publications (Palzewska, 1975, Noronha, *et al.*, 1999, Neri *et al.*, 2001, and Shen *et al.*, 2001) have reported that formation of Pd hydride depends on the particle size of palladium; larger Pd particles were more easily to form Pd hydride whereas smaller Pd particle may be unable to form Pd-β-hydride phase.

Under certain conditions, Pd-β-hydride phase can appear as a soft material with higher mechanical abrasion (Alber *et al.*, 2001). This may be a reason that larger Pd particles of the catalyst granules form the Pd-β hydride phase that is leached from the

catalysts. The results in this study were found to be in agreement with the previous works reported by our group that large Pd particles on silica supports were leached during liquid phase hydrogenation reaction (Panpranot *et al.*, 2004). Recently, Mastalir *et al.* (2004) showed that Pd-β-hydride phase was catalytically inactive for hydrogenation reaction. It is also known that keeping palladium crystallites in a well-reduced, metallic state can prevent formation of soluble complex compounds during liquid phase hydrogenation reactions (Bird *et al.*, 1980).

Table 5.6 Results from Atomic Adsorption.

Catalyst	**% Pd loaded (wt.%)**		**% metal loss**
	Fresh	**Spent**	
$Pd(OAc)_2/SiO_2$	0.33	0.21	36.36
$Pd(NO_3)_2/SiO_2$	0.44	0.26	40.91
$PdCl_2/SiO_2$	0.57	0.56	1.75
$Pd(OAc)_2$/MCM-41	0.41	0.28	31.71
$Pd(NO_3)_2$/MCM-41	0.34	0.20	41.18
$PdCl_2$/MCM-41	0.47	0.46	2.13

* After hydrogenation of 1-hexene (30^oC, 1 atm. and 1-hexene/ethnol = 1:7)

Hydrogenation activity of the leached Pd remaining in the solution was investigated using the following procedure.

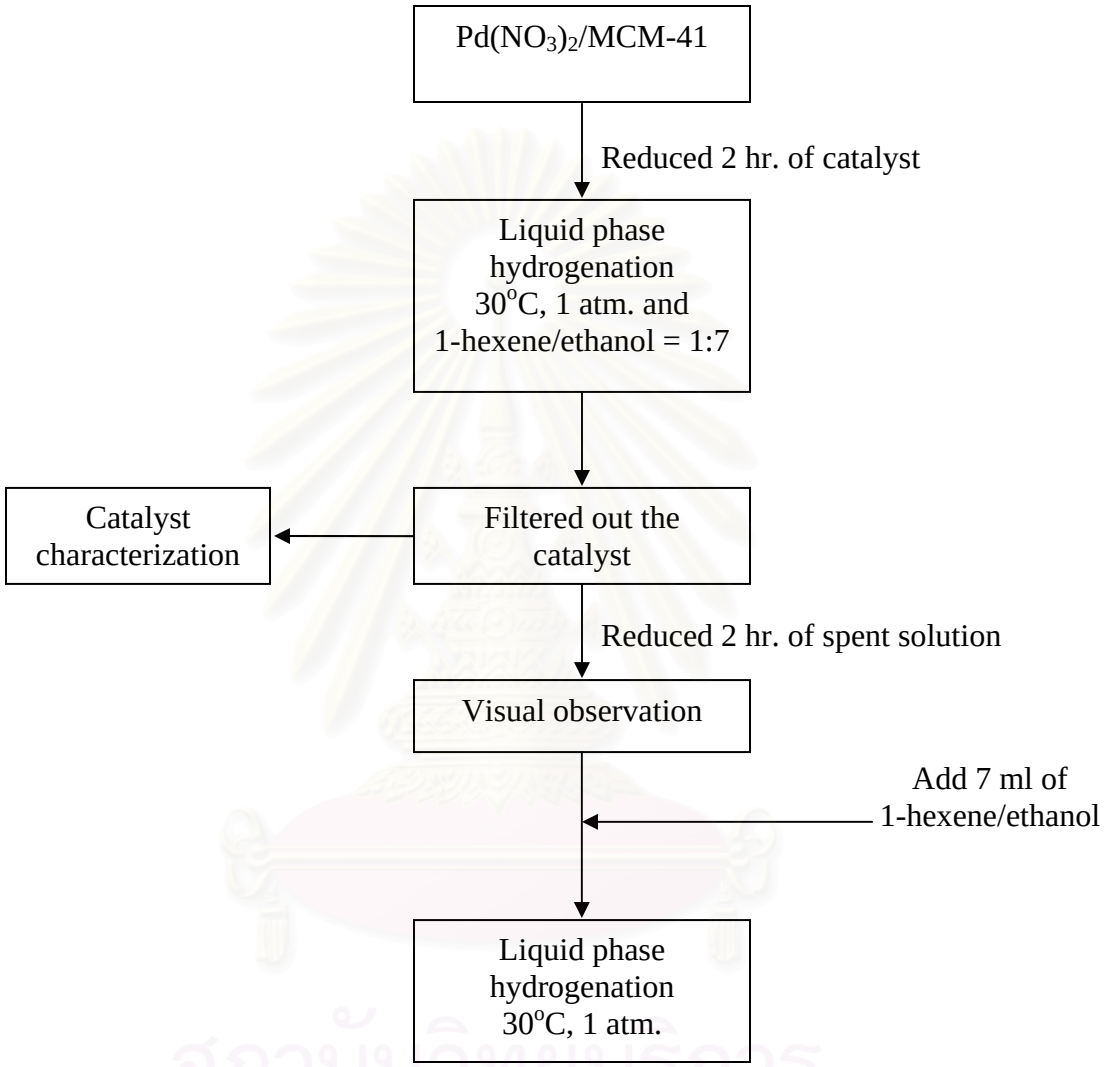

After filtered out the catalyst and re-reduced in H_2, no Pd^0 metal (Pd black) was found in the spent solution. No catalytic activity for hydrogenation of 1-hexene was observed. Thus, it is likely that the leached Pd was in a catalytically inactive form and/or the leached Pd was re-deposited onto the catalyst surface after reaction.

5.2.6 CO-Pulse Chemisorption

Chemisorption is the relatively strong, selective adsorption of chemically reactive gases on available metal sites or metal oxide surfaces at relatively higher temperatures (i.e. 25-400°C); the adsorbate-adsorbent interaction involves formation of chemical bonds and heats of chemisorption in the order of 50-300 kJ mol^{-1}.

Since H_2 chemisorption on Pd bridge bonding may occur so there is no precise ratio of atom to Pd metal surface. H/Pd stiochiometry may be varied from 1, 1/2 or 1/3. However, for CO chemisorption, CO/Pd stiochiometry is normally equal to 1. Exposed active surface areas of Pd of the catalysts were calculated from the irreversible pulse CO chemisorption technique based on the assumption that one carbon monoxide molecule adsorbs on one palladium site (Mahata and Vishwanathan, 2000, Ali and Goodwin, 1998, Sales *et al.*, 1999, Sarkany *et al*., 1993, Vannice *et al.*, 1981, and Nag, 1994). The amounts of CO chemisorption on the catalysts, the Pd dispersion, and the Pd metal particle sizes are given in Table 5.6. For the fresh catalysts, dispersion of Pd on both SiO_2 and MCM-41 supports varied in the order of $PdCl_2 > Pd(OAc)_2 \approx Pd(NO_3)_2$. The average particle sizes for reduced Pd^0 were reported and were calculated to be in the range of 3.5-7.0 nm with $PdCl_2$ on SiO_2 resulted in the smallest Pd^0 particle size. These average Pd metal particle sizes calculated based on CO chemisorption are not identical to the PdO particle sizes determined by XRD and TEM. Although comparing the BET surface areas of the original supports, MCM-41 has higher surface area than SiO_2, for any given type of Pd precursor used, the amounts of CO chemisorption of Pd/SiO_2 catalysts were found to be higher than those of Pd/MCM-41. The results suggest that the reducibilities of MCM-41 supported catalysts may be lower than of those of SiO_2 supported ones similar trend was also observed by Koh *et al*. (1997) that Pd/MCM-41 was only 70% reducible at room temperature.

In our study, Pd catalysts prepared from $PdCl_2$ exhibited high CO chemisorption and high Pd dispersion, therefore, the amount of residual chloride blocking active sites was minimal. However, there have been some cases in the literature reported that residual chloride remained on supported Pd catalysts and their catalytic activities of the catalysts were reduced (Mahata *et al.,* 2000).

After reaction the number of active sites measured by CO chemisorption was decreased ~ 50 % for all the catalysts samples as shown in the previous section, the decrease in the number of active sites of silica supported palladium catalysts were due to Pd leaching, Pd sintering, and probably coke deposition on the catalysts. Smaller Pd particles (from $PdCl_2$) were found to exhibit greater metal sintering while leaching occurred to a significant degree on larger particles (from $Pd(NO_3)_2$ and $Pd(OAc)_2$) Sintering of metal particles results in loss of active surface area and is usually an irreversible catalyst deactivation (Bergeret and Gallezot, 1997). The sintering of palladium in liquid phase hydrogenation has also been reported in the literature for other catalyst systems (Sermon, 1972, Schuurman *et al.*, 1992, Bakos *et al.*, 1997, Choudary *et al.*, 1999, and Dominguez-Quintero *et al.*, 2003. The contribution to the decrease in the number of active sites from Pd leaching is not clearly understood since leached Pd may be able to re-deposit to the support or itself was catalytically inactive. Coke formation varies from high-molecular weight hydrocarbons to primarily carbons such as graphite, depending upon the conditions under which the coke was form and aged (Farrauto and Bartholomew, 1997). Future study to determine the amount of carbon deposit on the catalysts is recommended.

The active sites of $PdCl_2$/MCM-41 were found to decrease the most after reaction. It is suggested that small Pd metal located in MCM-41 pore structure of the fresh catalyst may be occluded in the MCM-41 support when MCM-41 was partially collapsed during the reaction. Percent palladium dispersion for spent $Pd(OAc)_2$, $Pd(NO_3)_2$ catalysts, however, were not significantly changed from the fresh catalyst due to the total amounts of Pd remaining on the catalyst sample were also reduced by half from metal leaching. Percent palladium dispersion for spent Pd catalysts prepared from palladium chloride on

both SiO_2 and MCM-41 supports, however, decreased significantly since the total amount of Pd as confirmed by AAS was not changed. The Pd^0 particle sizes of $PdCl_2/SiO_2$ and $PdCl_2$/MCM-41 increased by approximately 50 and 100 % while those of the ones prepared from palladium acetate and palladium nitrate were slightly increased (~ 3-20 %). Large Pd metals on the spent $Pd(NO_3)_2$ and $Pd(OAc)_2$/MCM-41 catalysts were calculated due to lower amount of CO chemisorption

Table 5.7 Results from Pulse CO Chemisorption

Catalyst	Active sites[a] ($x10^{18}$ molecule/g)		% dispersion[b]		Pd^0 particle size[c] (nm)		%size increase
	Fresh	Spent	Fresh	Spent	Fresh	Spent	
$Pd(OAc)_2/SiO_2$	4.11	2.47	22.02	20.79	5.09	5.39	5.89
$Pd(NO_3)_2/SiO_2$	4.01	2.50	17.70	17.00	6.32	6.59	4.27
$Pd(Cl)_2/SiO_2$	8.40	5.37	26.05	17.00	4.30	6.61	53.75
$Pd(OAc)_2$/MCM-41	4.11	2.72	17.72	17.70	6.32	6.52	3.14
$Pd(NO_3)_2$/MCM-41	3.49	1.70	18.15	15.00	6.17	7.48	21.23
$Pd(Cl)_2$/MCM-41	8.03	3.80	30.20	14.60	3.71	7.67	106.82

[a] Error of measurement was ± 5%.

[b] Based on the total palladium loaded. An assumption of CO/Pd^0_s=1 was used where Pd^0_s is a reduced surface atom of Pd

[c] Based on d = (1.12/D) nm (Mahata and Vishwanathan, 2000), where D = fractional metal dispersion.

CO chemisorption of the catalyst after repeated reaction for 1-4 cycles was also investigated. After repeated 4 batches reaction experiments, it is shown that active sites of spent catalysts were slightly decreased from the first batch. However, active sites of

the forth batch were similar to the second batch. The CO chemisorption of spent catalysts may have reached a limiting value. The active sites of the spent $PdCl_2$ supported SiO_2 was still the highest ones among different supported Pd catalysts in this study. This suggests that $PdCl_2/SiO_2$ was the best palladium catalysts for liquid phase hydrogenation.

Table 5.8 Recycle of the catalyst

No. reaction	**Active sites ($x10^{18}$ molecule/g)**
0	8.03
1	3.8
2	-
3	-
4	3.11

* Reaction condition were 30^{o}C and 1 atm. and 1-hexene/ethanol = 1:7

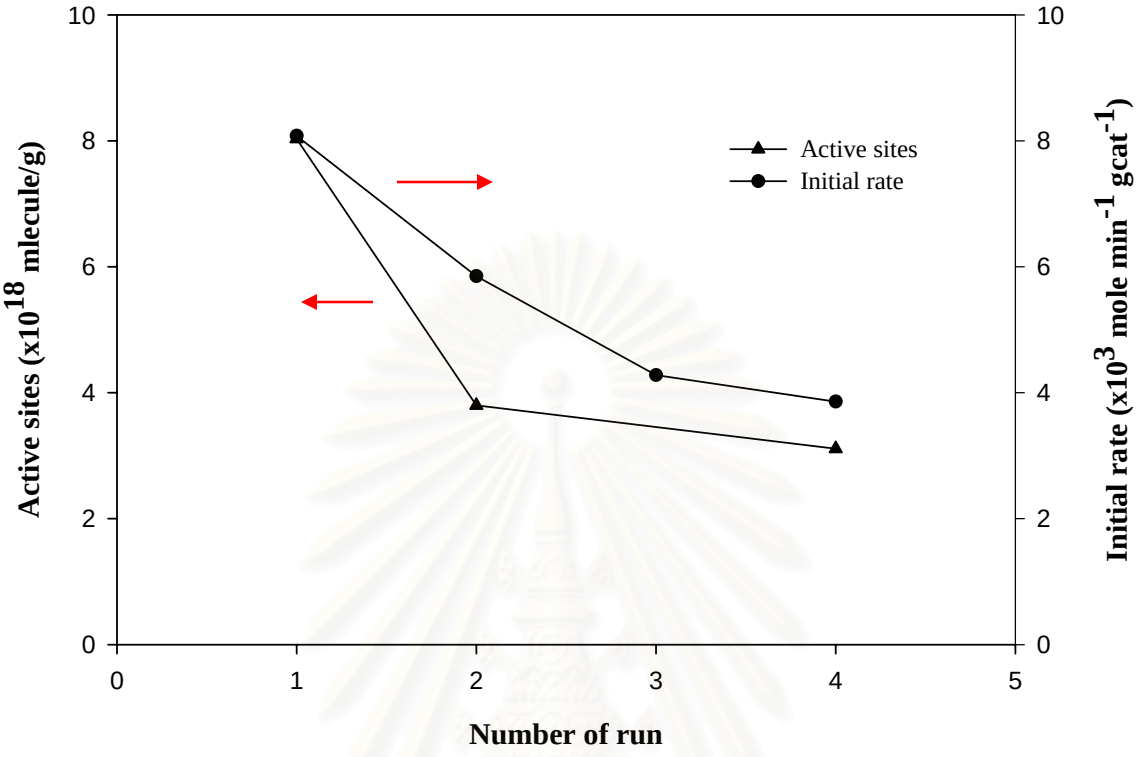

Figure 5.23 Stability of $PdCl_2$/MCM-41 as a function of number of reaction cycles (reaction condition: 30°C and 1 atm. and 1-hexene/ethanol = 1:7)

5.2.7 Temperature programmed reduction (TPR)

Temperature-programmed reduction is used to measure rate of reduction as a function of temperature at a linear temperature ramp. This technique provides the study of oxidation states of surface and bulk of a solid. Reducibility of a catalyst can be calculated from the area under the TPR profile.

The reducibility of the supported Pd catalysts is important since the active phase for hydrogenation is the metallic Pd^0 phase not its oxide. The H_2 consumption in TPR profile correspond to the reduction of $Pd^{2+} \longrightarrow Pd^0$, assuming that palladium is presented as PdO (H_2/Pd =1), which is the expected state for the preparation of the catalysts after calcinations step. TPR profiles of the MCM-41- and SiO_2-supported Pd catalysts are shown in Figures 5.23 and 5.24, respectively.

It was found that the catalysts reduced readily to PdH_2 once hydrogen was introduced to the system, which is typical for supported Pd catalyst (shen *et al.,* 2001). However, for MCM-41 supported catalysts, a small reduction peak at ca. 65^oC was observed for all the catalysts prepared with different Pd precursors. This peak is attributed to a portion of the PdO that could not be reduced at ambient temperature (Koh et al., 1997 and Ponpranot *et al.,* 2004). A significant negative peak at ca. 85^oC was observed for all the catalysts, this peak can be attributed to the decomposition of PdH_2 (Cubeiro *et al.,* 1998). The reducibilities of MCM-41 supported Pd catalysts were found to be only about 70% at ambient temperature (Koh *et al*. 1997). Due probably to the lower reducibility of MCM-41 supported catalysts, the catalysts prepared on MCM-41 exhibited only similar Pd dispersion and hydrogenation activities compared to those on SiO_2. It has also previously been reported that there is a stronger metal-support interaction between metal and an MCM-41 support when the pore size of that support is very small (i.e., 3 nm) (Panpranot *et al.,* 2002).

$$1.5\ H_2 + PdO \longrightarrow Pd^sH + H_2O \quad (1)$$

$$Pd^bH_x \longrightarrow Pd^b + 0.5xH_2 \quad (2)$$

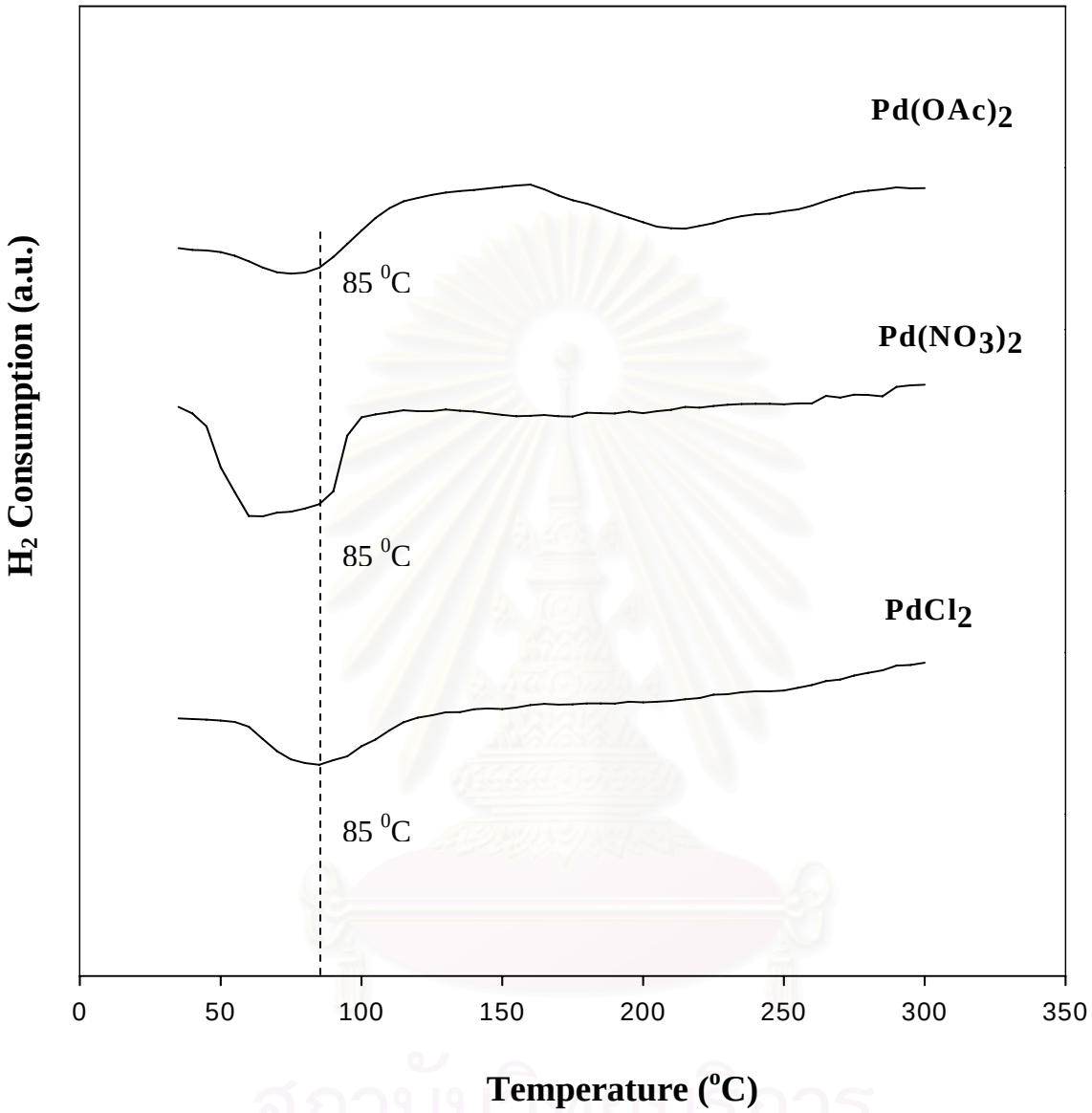

Figure 5.24 TPR profiles of the Pd/SiO_2 catalysts prepared with different Pd precursors.

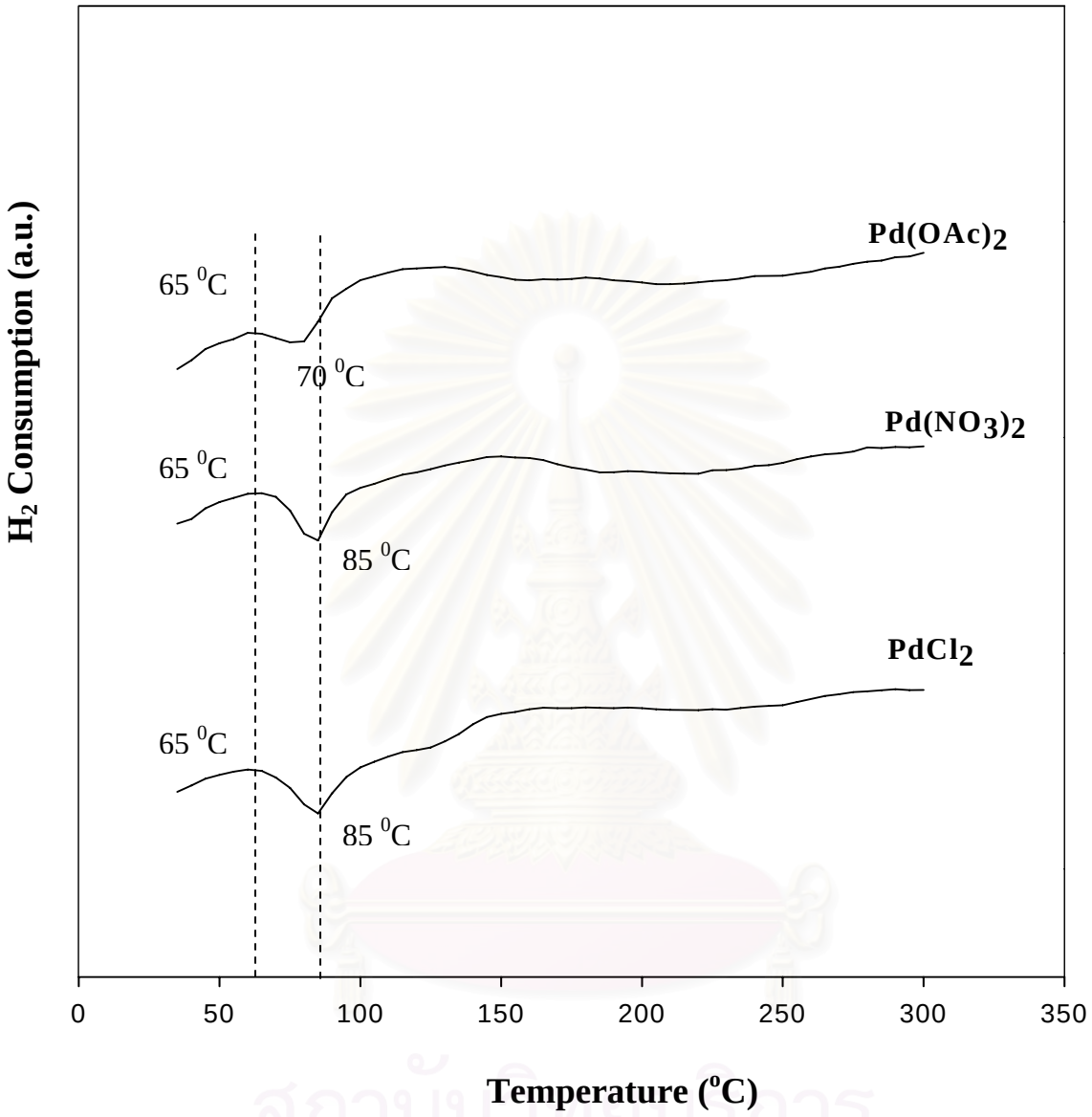

Figure 5.25 TPR profiles of the Pd/MCM-41catalysts prepared with different Pd precursors.

5.3 Effect of Reduction Temperature

The effect of reduction temperature on the CO chemisorption activity was investigated using the $PdCl_2/SiO_2$ catalyst since it showed the highest activity. The catalysts were reduced at a desired reduction temperature in the range of 30-300^oC. Typically, palladium catalyst can be easily reduced from Pd oxide to Pd metal phase at room temperature. The TPR profile of the catalysts is already shown in section 5.2.7. The measurement of active Pd metals by CO chemisorption technique was carried out. according to the CO chemisorption procedure explained in section 5.2.6. In Figure 5.25, the optimum reduction temperature for the $PdCl_2/SiO_2$ catalyst that maximized active surface palladium was determined to be around 150^oC. Higher reduction temperature may lead to decomposition of palladium hydride to palladium metal hence higher amount of activity of active palladium available for CO chemisorption. Thus, it is suggested that palladium hydride was inactive for the hydrogenation reaction. The results from this study were found to be in a good agreement with a recent work reported recently by Mastalir *et al.* (2004) that Pd-β-hydride phase was catalytically inactive for hydrogenation reaction. However reduction temperature too high may lead to sintering of palladium metal resulting in lower chemisorption activity. It should also be noted that silica supported palladium catalysts prepared from different palladium precursor catalysts do not necessarily have the same optimum reduction temperature.

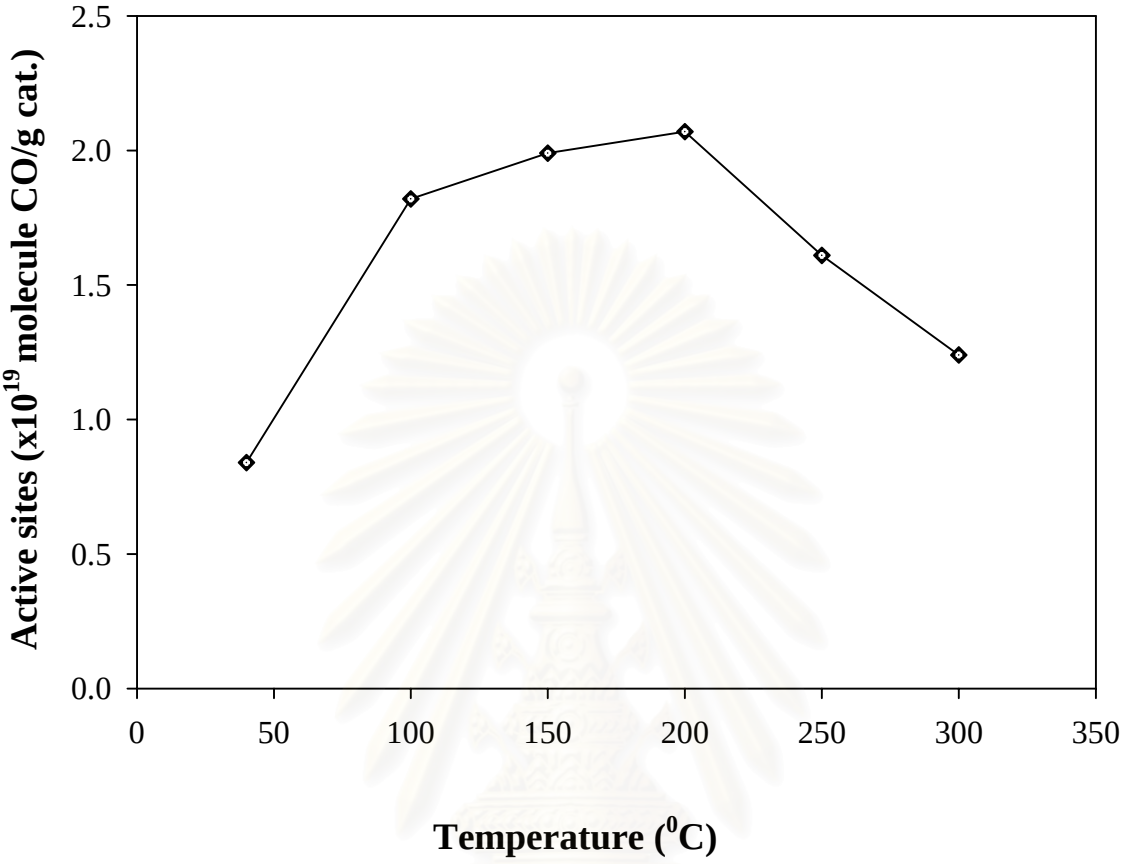

Figure 5.26 Plot of active sites measured by CO chemisorption of $PdCl_2/SiO_2$ catalysts vs. reduction temperature

CHAPTER VI

CONCLUSIONS AND RECOMMENDATIONS

6.1 Conclusions

In this study, the effect of Pd precursors on the dispersion of Pd on SiO_2 and MCM-41, the catalytic activities for liquid phase hydrogenation of the 1-hexene and deactivation of catalysts was extensively investigated. The following conclusions can be drawn:

1. By varying palladium precursors, different particle sizes of palladium were obtained on silica support. Palladium chloride precursor resulted in very small palladium particles, high Pd dispersion, and high hydrogenation activity for both SiO_2 and MCM-41 supports. On the other hand, Pd catalysts prepared from palladium acetate and palladium nitrate showed considerably large palladium particle sizes, low Pd dispersions and consequently low hydrogenation activities.

2. Silica supports (SiO_2 and MCM-41) did not have a significant impact on this reaction (support insensitive). However, the structure of MCM-41 was found to be partially collapsed after reaction for 1.5 hour.

3. The results suggest that deactivation of silica supported Pd catalysts in liquid phase hydrogenation was dependent on the palladium particle size. Smaller Pd particles were susceptible to sintering while larger particles were likely to be leached. An optimum Pd particle size may be needed in order to minimize such loss while enhance Pd dispersion.

4. The optimum reduction temperature for the $PdCl_2/SiO_2$ catalysts was determined to be ca. 150^oC. The results suggest that a complete decomposition of PdH_2 to Pd^0 increased the amount of active surface Pd as measured by CO chemisorption.

6.2 Recommendations

1. The mechanism for deactivation of metal catalyst due to metal leaching during liquid phase hydrogenation should be studied.

2. Different preparation techniques and/or Pd precursors may be tried in order to prepare high activity supported Pd catalysts with minimize Pd loss.

3. Further study should be performed using EDX technique.

References

Aramendia, M.A., Borau, V., Jimenez, C., Marinas, J., Porras, A. and Urbano, F.J. Selective Liquid-Phase Hydrogenation of Citral over Supported Palladium. J.Catal. 172 (1997): 46-54.

Corma, A. From Microporous to Mesoporous Molecular Sieve Materials and Their use in Catalysis. Chem. Rev. 97 (1997): 2373-2419.

Ali S. H.; and Goodwin J. G., SSITKA Investigation of Palladium Precursor and Support effects on CO Hydrogenation over Supported Pd Catalysts. J.Catal. 176 (1998): 3–13.

Alber, P.; Pietsch, J.; and Parker, S.F. Poisoning and deactivation of palladium catalyst. J. Mol. Catal. A 173 (2001): 275-286.

Bird, A. J.; Thompson, D. T.; and Jones (Ed.), in W. H. “Catalysis and Organic Synthesis”, Academic Press, London, 1980.

Besson, M.; and Gallezot, P. Deactivation of metal catalysts in liquid phase organic reactions Catal. Today 81 (2003): 547-559.

Cubeiro, M.L.; and Fierro, J.L.G. Partial Oxidation of Methanol over Supported Palladium Catalysts. Appl. Catal. A 168 (1998): 307-322.

Choudary, B.M.; Kantam, M.L.; Reddy, N.M.; Rao, K.K.; Haritha, Y.; Bhaskar, V.; Figueras, F.; and Tuel, A. Hydrogenation of acetylenics by Pd-exchanged mesoporous caterials. Appl. Catal. A. 181 (1999): 139-144.

Duca, D.; Liotta, L. F.; and Deganello G. Liquid phase hydrogenation of phenylacetylene on pumice supported palladium catalysts. J.Catal. 154 (1995): 69-79.

Dobrovolna, Z.; Kacer, P.; and Cerveny, L. Competitive hydrogenation in alkene-alkyne-diene systems with palladium and platinum catalysts. J.Mol.Catal. 130 (1998), 279-284.

Duvenhage, D.J.; and Coville, N.J. Fe:Co/TiO_2 bimetallic catalysts for the Fischer–Tropsch reaction Part 2. The effect of calcination and reduction temperature Appl.Catal. A: General 233 (2002) 63–75.

Quintero, O.D.; Martinez, S.; Henrequez, Y.; Ornelas, L.; Krentzien, H.; and Osuna, J. Silica-supported paladium nanoparticles show remarkable hydrogenation catalytic activity Jol.Mol.Catal. 197 (2003): 185-191.

Nazimek, D.; Bundyra, W.C. SSITKA Investigation of Palladium Precursor and

Support Effects on CO Hydrogenation over Supported Pd catalysts. Catal. Today. 90 (2004): 39–42.

Reichl, W.; and Hayek K. Vanadium Oxide Overlayers on Rhodium: Influence of the Reduction Temperature on the Composition and on the Promoting Effect in CO hydrogenation J. Catal. 208 (2002): 422–434

Farrauto, R.J.; and Bartholomew, C.H. “Fundamentals of Industrial Catalytic Processes” Kluwer Academic, 1997.

Gustafson, B.L.; and Lunsford, J.H. The Catalytic Reactions of Carbon Monoxide and Water over Ruthenium in a Y-Type Zeolite. J. Catal. 74 (1982): 393-404.

Gotti, A.; and Prins R. Basic Metal Oxides as Co catalysts for Cu/SiO_2 Catalysts in the Conversion of Synthesis Gas to Methanol J. Catal. 175 (1998): 302-311.

P. Johnston, R. W. Joyner, J. Influence of chlorine on the lability of small rhodium particles in carbon-monoxide Chem. Soc. Faraday Trans. 89 (1993): 863-864.

Jackson, S.D.; and Shaw, L.A. The liquid phase hydrogenation of phenyl acetylene and styrene on a palladium/carbon catalyst. Appl.Catal.A 134 (1996): 91-99.

Jackson, S.D.; Kelly, G.J.; Watson, S.R.; and Gulickx, R. Cycloalkene hydrogenation over palladium catalysts. Appl. Catal. A 187 (1999): 161-168.

Johnstone, Robert A.W., Liu, Jun-Yao, Lu, Ling and Whittaker, D. Hydrogenation of alkenes over palladium and platinum metals supported on a variety of metal (IV) phosphates. J. Mol. Catal. 191 (2002): 289-294.

Koningsberger, D.C.; Vaarkamp, M. Influence of the reduction temperature on the structure of the metal particles and the metal-support interface of $Pt/y\text{-}A1_20_3$ catalysts. Physical. B 208&209 (1995): 633-636.

Klug, H.P.; and Alexander, E. “X-Ray Diffraction Procedures For Polycrystalline Amorphous Materials 2nd ed.”, Wiley, New York, 1974.

Koh, C.A.; Nooney, R.; and Tahir, S. Characterisation and catalytic properties of MCM-41 and Pd/MCM-41 materials. Catal.Lett. 47 (1997): 199-203.

Marler, B.; Oberhagemann, U.; Vartmann, S.; and Gies, H. Influence of the sorbate type on the XRD peak intensities of loaded MCM-41. Microporous Mater. 6 (1996): 375-383.

Michalska, Z.M.; Ostaszewski, B.; Zientarska, J.; and Sobczak, J.W. Catalytic hydrogenation of alkadienes and alkynes by palladium catalysts supported on heterocyclic polyamides. J. Mol. Catal. 129 (1998): 207-218.

Mastalir, A.; Kiraly, Z.; and Berger, F. Comparative study of size-quantized Pd-montmorillonite catalysts in liquid-phase semihydrogenations of alkynes. Appl. Catal. A 269 (2004): 161-168.

Nag, N. K. A study on the dispersion and catalytic activity of gamma alumina-supported palladium catalysts. Catal. Lett. 24 (1994): 37-46.

Nozoe, T.; Tanimoto, K.; Takemitsu, T.; Kitamura, T.; Harada, T.; Osawa, T.; and Takayasu, O. Non-solvent hydrogenation of solid alkenes and alkynes with supported palladium catalyst. Solid State Ionics, 141 (2001): 695-700

Nishimura, S. "Handbook of Heterogeneous Catalytic Hydrogenation for Organic Synthesis", New York, 2001.

Mahata1, N.; and Vishwanathan, V. Influence of Palladium Precursors on Structural Properties and Phenol Hydrogenation Characteristics of Supported Palladium. Catalysts J. Catal. 196 (2000): 262–270

Palinko, I. Effects of surface modifiers on the liquid-phase hydrogenation of alkenes over silica-supported platinum, palladium and rhodium. Appl.Catal.A 126 (1995): 39-49

Pasqua, L.; Testa, F.; Aiello, R.; Renzo, F. Di.; and Fajula, F. Influence of pH and nature of the anion on the synthesis of pure and iron-containing mesoporous silica. Microporous and Mesoporous Mater. 44-45 (2001): 111-117.

Panpranot, J.; Goodwin, Jr., J.G.; and Sayari, A. Synthesis and characteristics of MCM-41 supported CoRu catalysts. Catal. Today 77 (2002): 269-284.

Panpranot, J.; Pattamakomsan, K.; Goodwin, Jr., J.G.; Praserthdam, P A comparative study of Pd/SiO_2 and Pd/MCM-41 catalysts in liquid-phase hydrogenation. Catal. Commun. 5 (2004): 583-590.

Panpranot, J.; Pattamakomsan, K.; Praserthdam, P.; Goodwin, Jr., J.G. Impact of Silica Support Structure on Liquid Phase Hydrogenation on Pd Catalysts. Ind. Eng. Chem. Res. in press. (2004)

Rylander, P.N. "Catalytic Hydrogenation over Platinum Metals", Academic Press, NY, 1967.

Rylander, P.N. "Hydrogenation Methods", Academic Press, London, 1985a.

Rylander, P.N. "Hydrogenation olefins Hydrogenation Methods", Academic Press, London, 1985b.

Sarkany, A.; Zsoldos, Z.; Furlong, B.; Hightower, J. W.; and Guczi, L. Hydrogenation of 1-Butene and 1,3-Butadiene Mixtures over Pd/ZnO Catalysts. J. Catal. 141 (1993):

566-582.

Schneider, M.; Wildberger, M.; Maciejewski, M.; Duff, D.G.; Mallat, T.; and Baiker, A. Preparation Structural Properties, and Hydrogenation Activity of Highly Porous Palladium-Titania Aerogels. J.Catal. 148 (1994): 625-638.

Sales, E.A.; Bugli, G.; Ensuque, A.; Mendes, M.J.; Bozon-Verduraz, F. Palladium Catalysts in the Selective Hydrogenation of Hexa-1,5-diene and Hexa-1,3-diene in the Liquid Phase. Effect of Tin and Silver Addition-Part 1. Preparation and Characterization: From the Precursor Species to the Final Phases. Chem. Phys. 1 (1999): 491-498.

Shen, W. J.; Ichihashi, Y.; Okumura, M.; Matsumura, and Y. Methanol synthesis from carbon monoxide and hydrogen catalyzed over Pd/CeO_2 prepared by the deposition-precipitation method Catal. Lett. 64 (2000): 23-25.

Shen, W. J.; Ichihashi, Y.; Ando, H.; Matsumura, Y.; Okumura, M.; and Haruta, M. Effect of reduction temperature on structural properties and CO/CO_2 hydrogenation characteristics of a $Pd\text{-}CeO_2$ catalyst", App. Catal. A: General 217 (2001): 231–239.

Shen, W. J.; Okumura, M.; Matsumura, Y.; and Haruta, M. The influence of the support on the activity and selectivity of Pd in CO hydrogenation. Appl. Catal. A 213 (2001): 225-232.

Shen, W.J.; Ichihashi, Y.; Ando, H.; Okumura, M.; Haruta, M.; and Matsumura, Y. Influence of palladium precursors on methanol synthesis from CO hydrogenation over Pd/CeO2 catalysts prepared by deposition-precipitation method. Appl. Catal. A 217 (2001): 165-172.

Sheldon, R.A.; and Bekkum, H.V. "Fine Chemicals through Heterogeneous Catalysis", Publ. Wiley-VCH, 2001.

Singh, U.K.; and Vannice, M.A. Liquid-Phase Citral Hydrogenation over SiO_2-Supported Group VIII Metals J.Catal. 199 (2001): 73-84

Shimazu, S.; Baba, N., Ichiku, N.; and Uematsu, T. Regioselective hydrogenation of dienes catalyzed by palladium-aminosilane complexes grafted on MCM-41. J. Mol.Cal 182 (2002): 343-350.

Tanaka, S.; Mizukami, F.; Niwa, S.; Toba, M.; Maeda, K.; Shimada, H.; and Kunimori, K. Preparation of highly dispersed silica-supported palladium catalysts by a complexing agent-assisted sol-gel method and their characteristics. Appl.Catal.A 229 (2002): 165-174.

Wolfgang, R.; and Konrad, H. Vanadium Oxide Overlayers on Rhodium: Influence of the

Reduction Temperature on the Composition and on the Promoting Effect in CO Hydrogenation. J. Catal. 208 (2002): 422–434.

Zhao, F.; Murakami, K.; Shiraai, M.; and Arai, M. Recyclable Homogeneous/ Heterogeneous Catalytic Systems for Heck Reaction trough Reversible Transfer of Palladium Species between Solvent and Support. J. Catal. 194 (2000): 479-483.

APPENDIX A

CALCULATION FOR CATALYST PREPARATION

Preparation of 0.5%Pd/MCM-41 and 0.5%Pd/SiO_2 catalysts by the incipient wetness impregnation method are shown as follows:

Reagent: - Palladium(II)acetate, Molecular weight. = 224.50 g
- Palladium nitrate dihydrate, Molecular weight. = 266.42 g
- Palladium(II)chloride, Molecular weight. = 177 g
- Support: - MCM-41 and SiO_2

Example Calculation for the preparation of 0.5% $Pd(NO_3)_2$ /MCM-41 catalyst

Based on 100 g of catalyst used, the composition of the catalyst will be as follows:

Palladium = 0.5 g

MCM-41 = 100-0.5 = 99.5 g

For 1 g of catalyst

Palladium required = 1×(0.5/100) = 0.005 g

Palladium 0.005 g was prepared from $Pd(NO_3)_2 \cdot 2H_2O$ and molecular weight of Pd is 106.42

$$\text{the } Pd(NO_3)_2 \cdot 2H_2O \text{ content} = \frac{\text{MW of } Pd(NO_3)_2 \cdot 2H_2O \times \text{Palladium required}}{\text{MW of Pd}}$$

$$= (266.42/106.42)\times 0.005 = 0.0125 \text{ g}$$

Since the pore volume of the pure silica support is 1.8 ml/g and 0.78 ml/g for MCM-41 and SiO_2, respectively. Thus, the total volume of impregnation solution which must be used is 1.62 ml for MCM-41 and 0.7 ml for SiO_2 by the requirement of incipient wetness impregnation method, the de-ionised water is added until equal pore volume for dissolve Palladium (II) nitrate dehydrate.

APPENDIX B

CALCULATION OF THE CRYSTALLITE SIZE

Calculation of the crystallite size by Debye-Scherrer equation

The crystallite size was calculated from the half-height width of the diffraction peak of XRD pattern using the Debye-Scherrer equation.

From Scherrer equation:

$$D = \frac{K\lambda}{\beta \cos \theta} \qquad (B.1)$$

where D = Crystallite size, Å

K = Crystallite-shape factor = 0.9

λ = X-ray wavelength, 1.5418 Å for CuKα

θ = Observed peak angle, degree

β = X-ray diffraction broadening, radian

The X-ray diffraction broadening (β) is the pure width of a powder diffraction free from all broadening due to the experimental equipment. α-Alumina is used as a standard sample to observe the instrumental broadening since its crystallite size is larger than 2000 Å. The X-ray diffraction broadening (β) can be obtained by using Warren's formula.

From Warren's formula:

$$\beta = \sqrt{B_M^2 - B_S^2} \qquad (B.2)$$

Where B_M = The measured peak width in radians at half peak height.

B_S = The corresponding width of the standard material.

Example: Calculation of the crystallite size of Pd/MCM-41-large pore

The half-height width of 111 diffraction peak = 0.95^{o} (from the figure B.1)

= $(0.95x\pi)/180$

= 0.0165 radian

The corresponding half-height width of peak of α-alumina (from the Bs value at the 2θ of 34.08^{o} in figure B.2) = 0.00422 radian

The pure width, $\beta = \sqrt{B_M^2 - B_S^2}$

$= \sqrt{0.0165^2 - 0.00438^2}$

= 0.016 radian

B = 0.016 radian

2θ = 34.08^{o}

θ = 17.04^{o}

λ = 1.5418 Å

The crystallite size $= \frac{0.9x1.5418}{0.016\cos 17.04} =$ 90.07 Å

= 9.1 nm

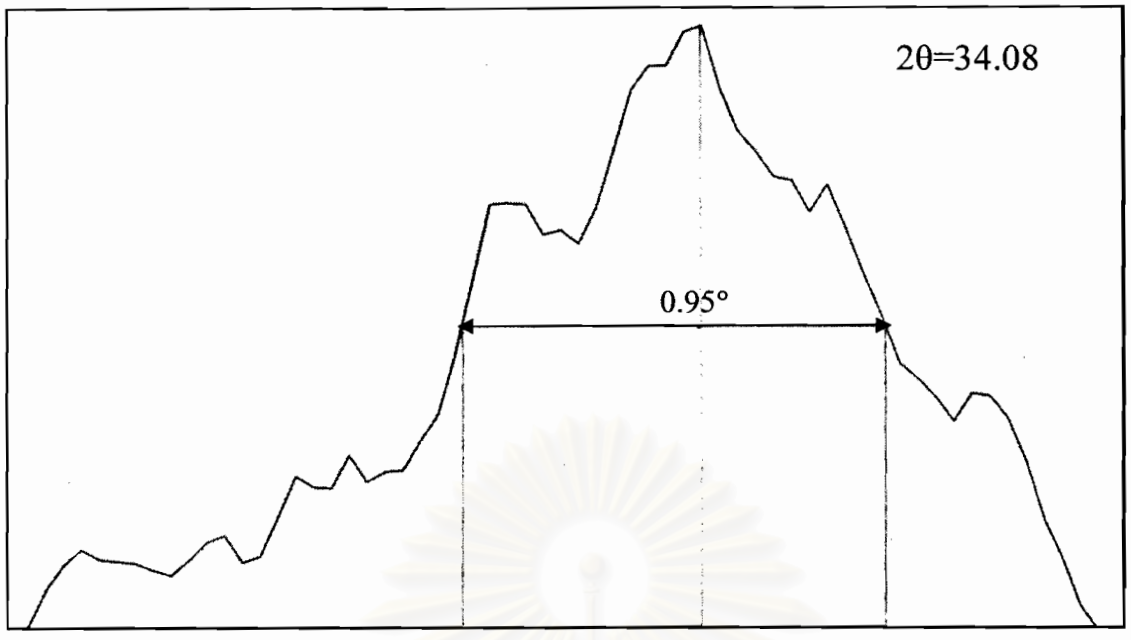

Figure B.1 The 111 diffraction peak of Pd/MCM-41-large pore for calculation of the crystallite size

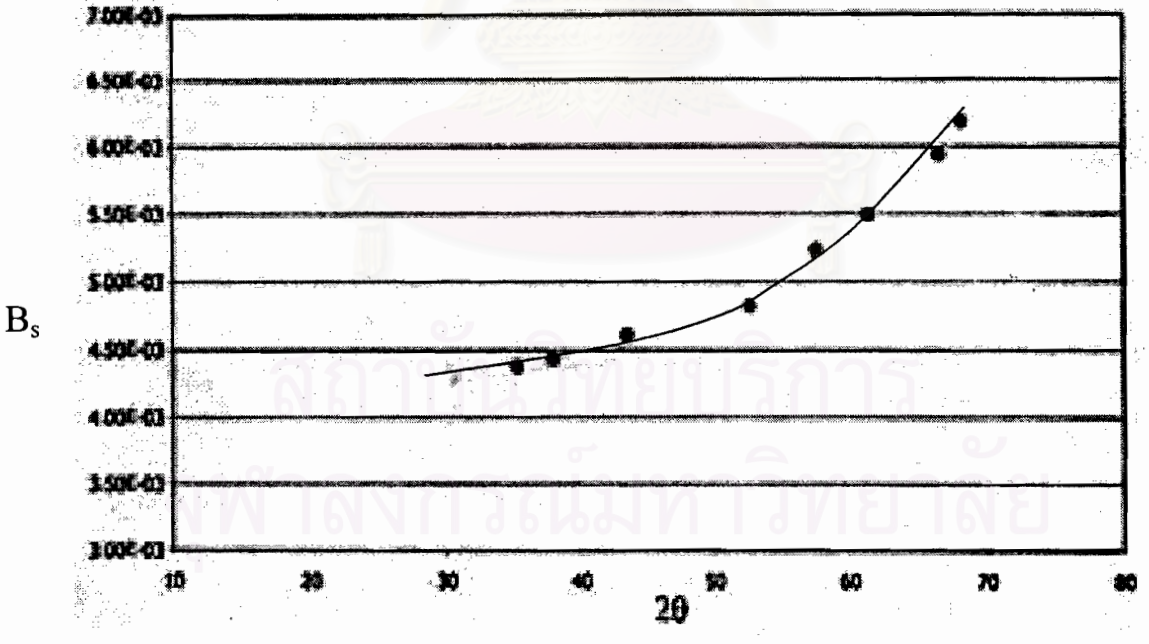

Figure B.2 The plot indicating the value of line broadening due to the equipment. The data were obtained by using α-alumina as a standard

APPENDIX C

CALCULATION FOR METAL ACTIVE SITES AND DISPERSION

Calculation of the metal active sites and metal dispersion of the catalyst measured by CO adsorption is as follows:

Let the weight of catalyst used	= W	g
Integral area of CO peak after adsorption	= A	unit
Integral area of 40 μl of standard CO peak	= B	unit
Amounts of CO adsorbed on catalyst	= B-A	unit
Volume of CO adsorbed on catalyst	= $40\times[(B-A)/B]$	μl
Volume of 1 mole of CO at 30°C	= 24.86×10^{6}	μl

Mole of CO adsorbed on catalyst = $[(B-A)/B]\times[40/24.86\times10^{6}]$ mole

Molecule of CO adsorbed on catalyst = $[1.61\times10^{-6}]\times[6.02\times10^{23}]\times[(B-A)/B]$ molecules

Metal active sites = $9.68\times10^{17}\times[(B-A)/B]\times[1/W]$ molecules of CO/g of catalyst

Molecules of Pd loaded = [%wt of Pd] $\times[6.02\times10^{23}]$/ [MW of Pd] molecules/g of catalyst

Metal dispersion (%) = $100\times$[molecules of Pd from CO adsorption/molecules of Pd loaded]

APPENDIX D

SAMPLE OF CALCULATION

D1 Calculation of Hydrogen consumed

The calculation of hydrogen consumed are as follow:

Let P = hydrogen consumed, psi

T = temperature during operation, K

V = volume of hydrogen stored tank, 0.283 L

R = 0.0821 L atm/mol K

n = mole of hydrogen

From ideal-gas equation

$$PV = nRT$$

$$n = PV/RT$$

$$n = \frac{P \text{ psi}}{14.7 \text{ psi}} \times \frac{1 \text{ atm}}{0.0821 \text{ L. atm}} \times \frac{0.283 \text{ L}}{T \text{ K}} \times \frac{\text{mol.K}}{}$$

$$n = 0.234P/T \quad \text{mol}$$

The molar volume of an ideal gas is 22.4 L at STP (0°C and 1 atm)

Hydrogen consumed = 0.234Px22.4/TL

$= 0.234Px22,400/T \quad cm^3$

D2 Calculation of Initial rate

At t = 5 min

Weight of catalysts = 0.1 g.cat

Initial rate = d mole $[H_2]/dt$

$$= \frac{(0.234P/T) \text{ [mole]}}{5 \text{ [min.] [g.cat.]}}$$

D3 Calculation of Turnover frequencies (TOF)

Metal active site = y molecule/g cat.

$$TOF = \frac{\text{rate}}{\text{(numbers of active site)}}$$

$$= \frac{\text{mole } H_2}{\text{[g cat.] [min]}} \Big| \frac{\text{[g cat.]}}{\text{y [active site]}} \Big| \frac{\text{[min]}}{\text{[s]}}$$

$$= [s^{-1}]$$

APPENDIX E

LIST OF PUBLICATION

Orathai tangjitwattanakorn, Joongjai Panpranot, and Piyasan Praserthdam "Liquid phase hydrogenation on silica supported Pd catalysts: Effects of Pd precursors and reduction temperature", Proceedings of the Regional Symposium on Chemical Engineering 2004, Bangkok, Thailand, Dec.1-3, 2004, Ref.No. NS-017.

VITA

Miss Orathai Tangjitwattanakorn was born in December 22th, 1981 in Bangkok, Thailand. She finished high school from Nualnoradit School, Bangkok in 1999, and received bachelor's degree in Chemical Engineering from the department of Chemical Technology, Faculty of Science, Chulalongkorn University, Bangkok, Thailand in 2003.